Cryovolcanism on Titan: New results from Cassini RADAR and VIMS

R. M. C. Lopes,[1] R. L. Kirk,[2] K. L. Mitchell,[1] A. LeGall,[3] J. W. Barnes,[4] A. Hayes,[5] J. Kargel,[6] L. Wye,[7] J. Radebaugh,[8] E. R. Stofan,[9] M. A. Janssen,[1] C. D. Neish,[10] S. D. Wall,[1] C. A. Wood,[11,12] J. I. Lunine,[5] and M. J. Malaska[1]

Received 20 August 2012; revised 28 January 2013; accepted 8 February 2013; published 19 March 2013.

[1] The existence of cryovolcanic features on Titan has been the subject of some controversy. Here we use observations from the Cassini RADAR, including Synthetic Aperture Radar (SAR) imaging, radiometry, and topographic data as well as compositional data from the Visible and Infrared Mapping Spectrometer (VIMS) to reexamine several putative cryovolcanic features on Titan in terms of likely processes of origin (fluvial, cryovolcanic, or other). We present evidence to support the cryovolcanic origin of features in the region formerly known as Sotra Facula, which includes the deepest pit so far found on Titan (now known as Sotra Patera), flow-like features (Mohini Fluctus), and some of the highest mountains on Titan (Doom and Erebor Montes). We interpret this region to be a cryovolcanic complex of multiple cones, craters, and flows. However, we find that some other previously supposed cryovolcanic features were likely formed by other processes. Cryovolcanism is still a possible formation mechanism for several features, including the flow-like units in Hotei Regio. We discuss implications for eruption style and composition of cryovolcanism on Titan. Our analysis shows the great value of combining data sets when interpreting Titan's geology and in particular stresses the value of RADAR stereogrammetry when combined with SAR imaging and VIMS.

Citation: Lopes, R. M. C., et al. (2013), Cryovolcanism on Titan: New results from Cassini RADAR and VIMS, *J. Geophys. Res. Planets*, *118*, 416–435, doi:10.1002/jgre.20062.

1. Introduction

[2] Data from the Cassini mission have revealed that Titan is a complex world in which interior, surface, and atmospheric processes interact to create and modify geologic features. In terms of active or recent surface-shaping processes, Titan is one of the most earthlike worlds in the solar system, often being referred to as the Earth of the outer solar system. Among the varied surface features observed by Cassini instruments are vast dune fields [e.g., *Radebaugh et al*., 2008], lakes [e.g., *Stofan et al*., 2006], fluvial channels [e.g., *Lorenz et al*., 2008], mountains [e.g., *Radebaugh et al*., 2007], and features that have been interpreted as volcanic [e.g., *Lopes et al*., 2007]. Alternate, exogenic interpretations for some putative volcanic features have been suggested [*Moore and Pappalardo*, 2011; *Moore and Howard*, 2010], particularly as new data have shown that Ganesa Macula, observed in Synthetic Aperture Radar (SAR) data and interpreted as a volcanic dome [*Elachi et al*., 2005; *Lopes et al*., 2007], does not have the topographic characteristics of a pristine dome [*Kirk et al*., 2008, 2009; *Lopes et al*., 2010a]. These new data have motivated the reexamination of possible volcanic features on Titan using data from the Cassini RADAR and Visible and Infrared Mapping Spectrometer (VIMS) instruments. In particular, new topographic information obtained from radargrammetry [*Kirk et al*., 2010] and SARTopo [*Stiles et al*., 2009] are used to reassess interpretations of volcanic features.

[3] Planetary volcanism has been defined by *Lopes et al*. [2010b] as an eruption from an opening on a planetary surface from which magma, defined for that body as a partial melt product of mantle or crustal material, is erupted.

[1]Jet Propulsion Laboratory, California Institute of Technology, Pasadena, California, USA.
[2]Astrogeology Science Center, United States Geological Survey, Flagstaff, Arizona, USA.
[3]Laboratoire Atmospheres, Milieux, Observations Spatiales (LATMOS), Universite Versailles Saint Quentin, Guyancourt, France.
[4]Department of Physics, University of Idaho, Moscow, Idaho, USA.
[5]Astronomy Department, Cornell University, Ithaca, New York, USA.
[6]Department of Hydrology and Water Resources, University of Arizona, Tucson, Arizona, USA.
[7]Department of Geophysics and Department of Electrical Engineering, Stanford University, Stanford, California, USA.
[8]Department of Geological Sciences, Brigham Young University, Provo, Utah, USA.
[9]Proxemy Research, Laytonsville, Maryland, USA.
[10]NASA Goddard Space Flight Center, Greenbelt, Maryland, USA.
[11]Planetary Science Institute, Tucson, Arizona, USA.
[12]Center for Educational Technologies, Wheeling Jesuit University, Wheeling, West Virginia, USA.

Corresponding author: R. M. C. Lopes, Jet Propulsion Laboratory, California Institute of Technology, Pasadena, CA 91109, USA. (Rosaly.M.Lopes@jpl.nasa.gov)

2169-9097/13/10.1002/jgre.20062

Volcanism that occurs on the outer solar system's satellites, sometimes known as cryovolcanism, is primarily the eruption of aqueous or nonpolar molecular solutions or partly crystallized slurries derived from partial melting of ice-bearing materials [*Kargel*, 1995]. We consider the eruption of water-melts from the interiors of icy satellites onto their surfaces as examples of volcanism, analogous to the familiar terrestrial process despite the lack of direct terrestrial material analogs on Earth [*Croft et al*., 1988].

[4] Early evidence for cryovolcanism was provided by Voyager 2 images of cratered rifts and smooth floors of filled depressions on Neptune's moon Triton, likely solidified water or methane ice melts [e.g., *Croft et al*., 1995]. Features on Europa and Ganymede may also have been formed by cryovolcanic activity [e.g., *Prockter*, 2004]. Cassini has revealed active plumes at Enceladus [e.g., *Porco et al*., 2006] emitted from fractures near the south pole that are warmer than their surroundings [*Spencer et al*., 2006], showing that Enceladus is presently active, although no features have been detected that indicate cryomagmas have come to the surface. Putative cryovolcanic features on Titan have been discussed using both RADAR data [e.g., *Elachi et al*., 2005, 2006; *Lopes et al*., 2007; *Stofan et al*., 2006; *Wall et al*., 2009; *Mitri et al*., 2008; *Lopes et al*., 2010a] and VIMS data [*Sotin et al*., 2005; *Le Corre et al*., 2009; *Soderblom et al*., 2009]. The possibility that cryovolcanism, or at least outgassing, is still active on Titan has been proposed by *Nelson et al*. [2009a, 2009b]; however, *Soderblom et al*. [2009] have argued that the brightness variations reported by Nelson et al. are not indicative of surface activity.

[5] Favorable conditions for cryovolcanism on Titan (summarized by *Lopes et al*. [2007]) include the likely existence of a liquid layer in Titan's interior, with some models placing it at 50–100 km depth [e.g., *Stevenson*, 1992; *Grasset and Sotin*, 1996; *Grasset et al*., 2000; *Tobie et al*., 2005, *Mitri et al*., 2008; *Nimmo and Bills*, 2010]. Recent results from Cassini radio science observations [*Iess et al*., 2012] show large crustal tides on Titan that can be explained in whole or in part by the presence of a global liquid ocean under the surface, most plausibly primarily of water.

[6] Thermal convection can occur in the stagnant lid regime in Titan's ice-I shell [*McKinnon*, 2006; *Mitri and Showman*, 2005; *Mitri et al*., 2008] while it is floating on an ammonia-water ocean [*Grasset and Sotin*, 1996; *Grasset et al*., 2000; *Tobie et al*., 2005; *Mitri et al*., 2008]. *Mitri et al*. [2008] showed that ammonia-water mixtures may erupt from a subsurface ocean on Titan through the ice shell, leading to cryovolcanism. They proposed that cryovolcanism may be related to fracturing in the ice crust overlying the ocean, which together with convection may lead to upward transport of ammonia-water fluid to the quiescent near-surface crust, where it refreezes and primes the crust for later episodes of volcanism. *Mitri et al*. [2008] also argued that, rather than steady state volcanism over the history of the solar system, cryovolcanism on Titan may have been confined to a late onset of convection in a cooling shell, and *Tobie et al*. [2005] proposed that it is episodically associated with fluctuations of heat flow associated with the evolution of the deep interior.

[7] Even if melting occurs, however, the eruption of ammonia-water would require a particular range of possible compositions that are not assured [*Kargel*, 1992]. If it does occur, ammonia-water cryovolcanism would likely behave much as basaltic volcanism does on Earth, with comparable construction of low-profile volcanic shields and other constructional volcanoes and flow fields [*Kargel*, 1992]. The potential for explosive cryovolcanism, as inferred and modeled for Triton [*Kargel and Strom*, 1990], is not clear for Titan; due to Titan's high atmospheric pressure, explosive events might be less common or less vigorous than in the case of basaltic volcanism on Earth [*Lorenz*, 1996]. On Titan, other cryolava compositions are possible, including saltwater solutions [*Kargel*, 1992], methanol-water [*Kargel*, 1992], and hydrocarbons [*Kargel et al*., 2010]. In this paper, we use morphological evidence to infer the origin of features. However, we recognize that caution is needed in interpretations, given the known differences between properties of familiar silicate and exotic cryovolcanic magmas [*Kargel et al*., 1991, 2010; *Kargel*, 1995; *Zhong et al*., 2009] and between Titan's and Earth's surface and crustal conditions and tectonic environments.

[8] The presence of methane (~5% at the surface) in Titan's atmosphere requires continued replenishment if its existence has persisted longer than about 10 million years [*Yung et al*., 1984], consistent with a methane-venting cryovolcanic process. The gas chromatograph mass spectrometer instrument on the Huygens probe detected the radiogenic isotope ^{40}Ar in Titan's atmosphere [*Niemann et al*., 2005, 2010]. This isotope is the product of ^{40}K decay (half-life 1.28 Gyr), and its presence, at a molar concentration in the atmosphere of 33.7 ppm [*Niemann et al*., 2010], equivalent to 48.5 ppm by mass, requires that this isotope has been vented from a reservoir containing the parent atom. However, *McKinnon* [2010] finds that the amount of degassing from the interior may be modest, and *Moore and Pappalardo* [2011] argue that alternative scenarios for Titan's atmospheric evolution are possibly viable. We agree that Titan's atmosphere contains only a small percentage of the satellite's global production of ^{40}Ar over geologic time, and therefore storage of degassed ^{40}Ar in clathrates or other surface or internal reservoirs (very likely), incomplete degassing (possible), or recent catastrophic atmospheric loss (improbable) are the possibilities. Regardless of argon's detailed history on Titan, cryovolcanism would be one means by which argon and methane might be brought to the surface.

[9] *Moore and Pappalardo* [2011] argued that Titan has a relatively inactive interior and that the surface features previously interpreted as cryovolcanic could be alternatively interpreted as being caused by fluvial or erosional processes. Considering available evidence, the question of whether cryovolcanism has taken place on Titan is still open. Therefore, we examine our data without using a priori assumptions about either the likelihood or improbability of cryovolcanism on Titan or about what its composition would be, if eruptions have taken place. Therefore, features currently seen on the surface could be interpreted as having a cryovolcanic, noncryovolcanic, or ambiguous origin. We examine the features that have been attributed to cryovolcanism and for which new data are available. In particular, the existence of topographic data and compositional maps from VIMS

can help to determine which class of processes (cryovolcanic or noncryovolcanic) is most likely to have produced these features. The identification of volcanism is based on an assumption that the eruptive emplacement of melts and partial melts onto the surface involves either formation of identifiable flow fields or positive relief constructs associated with vents (which can be point sources, line sources, or other simple geometries occurring either in isolation or in simple clusters), or eruption pits caused by explosive clearing of the vent area or subsidence related to cessation of volcanism. Keys to production of identifiable landforms, according to the definition of cryovolcanism, are of course that eruptions of fluids (with or without entrained solids and gases) occur and that the eruptive products produce solid deposits upon cooling. The processes and landforms are not necessarily exactly those produced by volcanism on Earth or other bodies, but the basic physical eruption physics and lava cooling/solidification provides reasonable constraints on the subjective identification process and understanding of what to look for.

2. Cassini Data Sets

2.1. Cassini RADAR: SAR Imaging and Topography

[10] Cassini carries a multimode Ku-band (13.78 GHz, $\lambda = 2.17$ cm) radar instrument [*Elachi et al*., 2005b] designed to map the surface of Titan and to observe other targets in the Saturn system in four operating modes—SAR, altimetry, scatterometry, and radiometry. Here we use Titan data obtained in the SAR mode, which is used at altitudes under ~4,000 km, resulting in resolutions ranging from ~350 m to >1 km (although the images are gridded uniformly at 175 m/pixel to preserve their resolving power even in the areas near closest approach where this is best). Images are acquired either left or right of nadir using two to seven looks. At each Titan encounter used by the RADAR, a swath 120–450 km wide and ranging from 1000 to 5000 km in length is created from five antenna beams, with coverage largely determined by spacecraft range and orbital geometry. Swaths are commonly referred to by the Titan flyby designation, starting with Ta (the first flybys were given letter designations) and continuing from T3 through T77 for the data used in this paper. Topographic data can be obtained from single SAR swaths or overlapping pairs by a variety of methods including radarclinometry (shape-from-shading, e.g., *Kirk et al*. [2005]), monopulse "SARTopo" processing [*Stiles et al*., 2009], and radar stereogrammetry [*Kirk et al*., 2008].

[11] Radar backscatter variations in SAR images can be interpreted in terms of variations of surface slope at the pixel scale, near-surface roughness at the wavelength scale, and near-surface dielectric properties (see discussion in *Stofan et al*. [2006]; *Lopes et al*. [2010a]). On Titan, the candidate surface materials include water ice, water-ammonia ice, and other ice mixtures, hydrocarbons, and nitriles and other C, N, H-bearing organics [e.g., *Soderblom et al*., 2007]. These are different from the rocky surfaces more usually imaged with radars; in particular, volume scattering at Titan may be particularly significant compared to rocky surfaces because of the much lower loss of the likely surface materials at Titan temperatures [e.g., *Janssen et al*., 2009]. Interpretation of SAR images and use of them as a basis for geological mapping is not straightforward; this has been discussed by *Stofan et al*. [2006] and *Lopes et al*. [2010a] specifically for Cassini SAR data. Therefore, we can expect that preliminary interpretations may have to be revised as more data (e.g., from different look angles or another type of data) become available. In particular, topographic data greatly help geologic interpretations.

[12] The SAR data of Titan used in this study (up to flyby T77, June 2011) comprise a rich data set that covers 48% of Titan's surface (excluding overlap), well distributed in latitude and longitude [*Lopes et al*., 2011]. Despite the Cassini RADAR having an altimetric mode, the total global coverage of altimetry data is sparse and generally not spatially correlated with SAR imagery. *Stiles et al*. [2009] devised a technique, based upon amplitude monopulse comparison [*Chen and Hensley*, 2005], that enables the extraction of additional topographic data that are not model-dependent or reliant on overlap between SAR swaths. The method estimates surface heights by comparing the calibration of overlapping Titan SAR imagery obtained from different antenna feeds of the RADAR instrument onboard the Cassini spacecraft, and as such is cospatial with the image data, yielding one to three profiles in each SAR pass that are ~9 km wide by thousands of kilometers long, extending along most of the long dimension of the SAR image strips. This technique has been validated by comparison with overlapping nadir-pointing radar altimetry. The comparison yielded an absolute bias of the height of 150 m [*Stiles et al*., 2009], and vertical resolution is ≤75 m. Because we obtain colocated SAR topography (henceforth referred to as SARTopo) along each SAR pass rather than only in regions with overlapping observations, the new technique extends the area of colocated topography and SAR imagery by an order of magnitude compared with stereo and nadir-pointing altimetry.

[13] Some overlapping images can be used for radar stereogrammetry as described by *Kirk and Howington-Kraus* [2008] and *Kirk et al*. [2008]. This method provides digital topographic models or DTMs with relatively high resolution (several kilometers horizontally and ~100 m vertically) over extended areas that are coregistered to the SAR image data. The areal coverage of DTM data permits three-dimensional visualization of the surface and hence greatly facilitates geologic interpretation. Radar stereogrammetry has the additional advantage of being based on rigorous geometric calculations rather than assumptions about the behavior of the surface at radar wavelengths, such as is necessary for radarclinometry [*Kirk et al*., 2005; *Radebaugh et al*., 2007; *Neish et al*., 2010]. From a geological point of view, it is particularly useful to have a DTM coregistered with SAR images. However, the overlapping image coverage required for stereo mapping is presently restricted to a few percent of Titan's surface. SARTopo has the advantage of providing topographic profiles across all SAR swaths. In this paper, we use both radar stereogrammetry and SARTopo results, where available, and combine topographic results with imaging from SAR to interpret the likely origin of candidate cryovolcanic features.

2.2. Cassini Radiometry Data

[14] The Cassini Radar can operate in a passive mode that provides unique insight into surface properties such as

overall composition, structure, and physical temperature. Radiometry data are acquired concurrently with active measurements or separately when the spacecraft is further than ~40,000 km away from Titan. Since the beginning of the Cassini mission, the radiometer has mapped the 2.2 cm thermal emission from almost the whole surface of Titan with resolution ranging from 5 to 500 km. The maps consist of global mosaics of the effective dielectric constant and equivalent brightness temperature at normal incidence. The calibration and mapping of the radiometry observations are described by *Janssen et al*. [2009]. The uncertainty on the dielectric constant is ~0.2. The brightness temperatures of Titan's surface are obtained with a relative precision of ~1 K and an absolute error of ~2 K.

[15] If there is active cryovolcanism on Titan, the "smoking gun" would be provided by the identification of a hot spot in the Cassini RADAR radiometry data (and, possibly, in VIMS data if temperatures were sufficiently high). Indeed, in the microwave domain (Rayleigh-Jeans regime), the brightness temperature T_b measured by the radiometer is related to the surface physical temperature T_{phys} through

$$T_b = eT_{\mathrm{phys}} \tag{1}$$

where e is the emissivity of the surface, i.e., its ability to radiate absorbed energy. The emissivity depends on both physical and chemical properties of the surface and near-surface. By definition, a black body under thermal equilibrium has an emissivity of 1, while a realistic surface has an emissivity lower than 1. The thermal emission from any surface is related to the radar reflectivity through Kirchhoff's law of thermal radiation: at thermal equilibrium, emissivity equals 1 minus the reflectivity. Using the radar active observations acquired concurrently with the passive measurements, we can thus compare the brightness temperature of a region to its reflectivity [*Janssen et al*., 2011b] and reveal a potential thermal anomaly. Equation (1) assumes that the propagation of the diurnal or seasonal thermal waves below the surface is negligible, i.e., that the physical temperature down to the depth sensed by the radiometer is that of the ground. This is due to the fact that only 10% of the solar flux reaches the surface of Titan through its thick atmosphere. The low solar fluxes and the huge thermal inertia of the atmosphere make unlikely the presence of diurnal temperature changes of much more than ~1 K [e.g., *Lorenz et al*., 2003; *Janssen et al*., 2009]. The physical ground temperature of Titan's surface is well known from Cassini's Composite Spectrometer (CIRS) observations [*Jennings et al*., 2009; *Cottini et al*., 2012] and the Huygens probe landing site measurements [*Fulchignoni et al*., 2005]: it is ~93.7 K at the Equator and decreases toward the poles by ~2–3 K. As illustrated by Figure 1, a hot spot would be a region characterized by a high brightness temperature (owing to a high physical ground temperature) that is either higher than the nominal physical temperature or inconsistent with the reflectivity. Several hot spots occurring in the same region would suggest a local thermal activity.

[16] To date, no hot spot has been unambiguously identified. However, the radiometry and scatterometry behaviors of the largest proposed cryovolcanic features listed in this paper have not been thoroughly investigated yet and will be addressed in [*Janssen et al*., 2011a]. Here, we highlight that the detection of thermal activity at Titan's surface using radiometry data is not straightforward for a number of reasons, including the following:

[17] (1) Cryovolcanic features may be sparse. As discussed below, only a few candidates have been proposed so far.

[18] (2) The radiometer resolution is at best 5 km, while the activity suggested by *Nelson et al*. [2009a, 2009b] is attributed to outgassing from fumarolic vents that are likely to be much smaller in area. Averaged on the radiometer footprint, the thermal signature of a hot spot could go unnoticed.

[19] (3) Water-rich cryolava on the surface of Titan would cool rapidly compared to the interval between Cassini observations, let alone in comparison to geologic time. The rate of cooling depends on the physical and thermal properties of

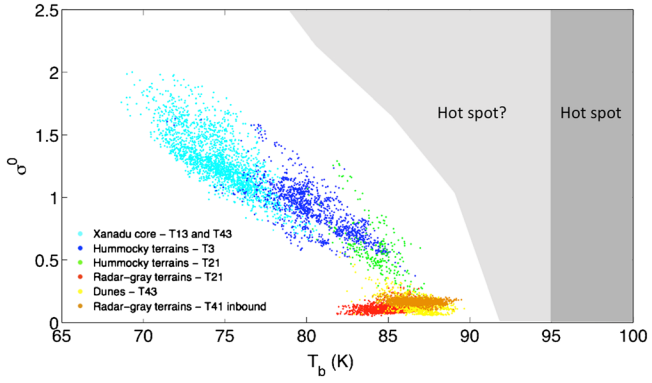

Figure 1. Scatter plot of brightness temperature versus normalized radar cross-section for selected regions on Titan, including the core of Xanadu, hummocky terrains, radar-gray plains, and dunes. These regions show different behaviors, Xanadu and the hummocky terrains being especially bright relative to their emissivity [*Janssen et al*., 2011b]. The shaded areas indicate where to search for putative hot spots. If T_b is larger than ~95 K, there is a definite thermal anomaly (dark gray shaded area). Otherwise, the consistency between T_b and σ^0 must be investigated (light gray shaded area). This figure is adapted from *Janssen et al*. [2011b].

the lava flow and the surface crust material and the properties of the atmosphere (density, temperature, and composition). On Titan, cooling is much faster than on airless icy moons; *Davies et al*. [2010] estimate that the surface temperature drops by ~50% within ~1 day of emplacement. Therefore, fresh cryolava flows may be difficult to detect unless an active eruption is directly observed.

[20] (4) Even if radiometry observations coincided with an active cryolava eruption, aqueous cryolavas [e.g., *Kargel*, 1995; *Lorenz*, 1996; *Nelson et al*., 2009a] would exhibit a high dielectric constant that would decrease the emissivity and offset a locally higher physical temperature, thus moderating the effect of a potential thermal event.

[21] Therefore, unambiguous detection of active volcanism might require the observation of surface change; none have been detected so far.

2.3. Cassini VIMS Data

[22] It is also possible to see the surface through Titan's haze at shorter wavelengths. Cassini's VIMS [*Brown et al*., 2004] maps the surface of Titan within eight near-infrared windows with wavelengths between 0.9 and 5.2 μm. Whereas this results in a discontinuous spectrum due to absorption by atmospheric methane between the spectral windows, the resulting data can identify variations in the nature of the surface across Titan and can help to constrain its composition [*Rodriguez et al*., 2006; *McCord et al*., 2008; *Clark et al*., 2010].

[23] VIMS data have been used to identify candidate cryovolcanic features Tortola Facula [*Sotin et al*., 2005] and Tui and Hotei Regios [*Barnes et al*., 2005; *Barnes et al*., 2006; *Nelson et al*., 2009a]. VIMS data were also used to complement other identifications like those in northern Fensal [*Le Corre et al*., 2009] and western Xanadu [*Wall et al*., 2009].

[24] Here we use VIMS observations from the T9 Cassini flyby of Titan to help evaluate the possibility that the region formerly known as Sotra Facula is the result of cryovolcanic processes (see *Barnes et al*. [2009] for a description of the VIMS Titan data set). We processed the data using the standard VIMS pipeline as outlined in *Barnes et al*. [2007a]. Lacking an effective atmospheric correction at present, we use calibrated I/F (specific intensity/solar flux) images to compare spectra of various surface units and limit our attention to observations with relatively small ($<30°$) emission angles. In particular, the greatest degree of surface variation is seen when using color maps in which the 5.0 μm band is mapped to red, 2.0 μm to green, and 1.28 μm to blue.

3. Candidate Cryovolcanic Features: New Data and Interpretations

[25] Topographic data acquired and analyzed since the first interpretations were made of putative cryovolcanic features are, we find, critical for the reinterpretation of these features. Three types of features on Titan have previously been interpreted as cryovolcanic in origin:

[26] (1) Apparent volcanic constructs associated with flow-like features, such as Ganesa Macula [*Elachi et al*., 2005; *Lopes et al*., 2007]; Tortola Facula [*Sotin et al*., 2005]; and the region formerly known as Sotra Facula [*Lopes et al*., 2010a].

[27] (2) Flow-like features not associated with a specific construct or candidate vent area. These include Rohe, Winia, and Ara Fluctus [*Lopes et al*., 2007]; a flow in the T3 SAR swath [*Lopes et al*., 2007; *Le Corre et al*., 2009]; and flow deposits in Tui Regio [*Barnes et al*., 2006], Hotei Regio [*Nelson et al*., 2009b, *Wall et al*., 2009; *Soderblom et al*., 2009], Western Xanadu [*Wall et al*., 2009], and flow deposits similar in morphology to these in T7 SAR and southern terrain SAR images.

[28] (3) Depressions that appear similar to calderas or pits, sometimes associated with flow-like features, such as Mohini Fluctus (in the region formerly known as Sotra Facula), and those associated with Rohe Fluctus and Ara Fluctus [*Lopes et al*., 2007].

[29] We discuss these features in light of both new data and suggested alternative interpretations, such as the fluvial hypothesis put forward by *Moore and Pappalardo* [2011]. Many of the latter features are flow-like, such as those found in Hotei or Tui. The origin of flow-like features is particularly difficult to ascertain, as such features could be fluvial or caused by mass movement and be morphologically similar. In particular, some sedimentary deposits (especially mass flows) and cryovolcanic flows are likely to have many geomorphologic similarities, including lobate boundaries, rough or variable backscatter surfaces, and multiple, overlapping deposits. Given that both are deposits produced by the flow of material, what criteria can be developed to distinguish their mode of origin?

[30] *Source type*. Channels can be produced by cryovolcanic, fluvial, and mass wasting processes; however, analysis of channel characteristics (lack of association with other volcanic features such as edifices, apparent drainage from higher standing terrain) can help to constrain channel origin. In addition, both sedimentary and volcanic processes can be active in a single region, either contemporaneously or not, resulting in the presence of fluvial or debris (mass wasting) channels near or within a lava flow field. Therefore, careful analysis of the relationship between flow units and channels is required. If flow features emerge directly from a channel that has sourced from a mountainous region, it is likely these are debris flows from fluvial runoff. If the flow originates from a fissure or circular feature (such as proposed for Rohe Fluctus [*Lopes et al*., 2007]), a cryovolcanic origin is more likely. If there are no channels or other fluvial features apparent in the region, a fluvial origin is not likely.

[31] The ability to distinguish fluvial from volcanic channels depends largely on spatial resolution (assuming that the geologic setting makes both types plausible). Examples of volcanic, fluvial, and debris channels are shown in Figure 2. Volcanic channels do not show dendritic patterns that are common on fluvial channels; however, these patterns may not be distinguishable in our data due to limited spatial resolution.

[32] *Topography*. Sedimentary and cryovolcanic deposits are most likely to be located in topographic lows and exhibit embayment relations with higher ground, but both may also occupy topographic highs and trend downslope. Subsequent to deposition, sedimentary deposits and volcanic flows can

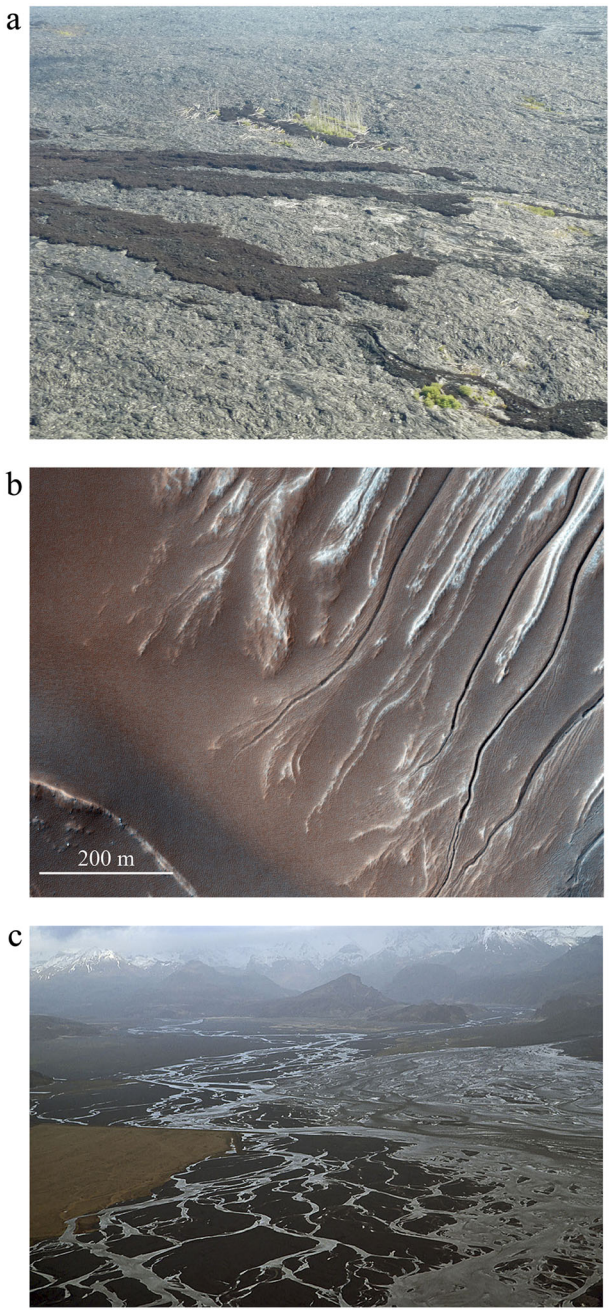

Figure 2. Morphological differences in lava, debris, and fluvial channels are apparent. (a) Basaltic lava flows from Kilauea volcano, Hawaii. Rough 'a'a (dark) and smooth pahoehoe (gray) surfaces are created from lavas of roughly similar composition. Note lobate flow margins and levees. Trees indicate scale; the image is about 300 m across. Aerial photo from Jani Radebaugh. (b) Avire Crater debris flow deposits, Mars. The flows producing these deposits are probably slightly less viscous than the basaltic lavas in Figure 2a. Note the levees. Courtesy of NASA/University of Arizona, MRO HiRISE image ESP_023322_1390. (c) Braided fluvial channels in glacial outwash plain below Eyjafjallajökull, Iceland. Eruptions released glacial water onto the plain below in a large outflow. Image is about 5 km across. Photo by Marco Fulle, 2010.

be affected by erosion and be left standing as perched deposits and inverted landscapes [e.g., *Pain et al*., 2007; *Burr et al*., 2010]. Thickness of a volcanic flow can be a discriminator; the work of *Kargel et al*. [1991] showed that mixtures such as ammonia-water and ammonia-water-methanol can exhibit a range of rheologies that overlaps the range for silicate flows. In contrast, fluvial sedimentary deposits generally only have significant thickness if they pond in a depression or aggrade in thick alluvial fans or form thick debris flows [e.g., *Nichols*, 2009]. Debris flows and volcanic flows in particular can be geomorphologically similar, as both may be leveed.

[33] Below we reexamine the major features and areas previously identified as cryovolcanic using new topographic data and assessing whether a fluvial or other origin is likely, given, for example, the presence or absence of channels.

3.1. Ganesa Macula

[34] This radar-dark feature with some bright edges centered at 87.3°W, 50.0°N has a circular appearance in SAR data and was originally interpreted as a cryovolcanic dome or shield, perhaps similar to steep-sided domes on Venus [*Elachi et al*., 2005; *Lopes et al*., 2007]. The existence of steep-sided ("pancake") domes on Titan had been predicted [*Lorenz and Mitton*, 2002] on the basis that the likely percentage of methane as volatile dissolved in cryomagmas would not be sufficient at Titan's atmospheric pressure to produce explosive eruptions [*Lorenz*, 1996]. The similar appearance of Ganesa and Venus domes in SAR data (see Fig. 3 in *Lopes et al*. [2007]) together with the favorable conditions for their formation on Titan led to the initial interpretation of Ganesa's origin. However, profiles obtained by *Stiles et al*. [2009] using SARTopo did not show Ganesa's topographic profile to be that of a dome or shield. Once data from flyby T23 were acquired, providing the needed overlap with the swath from flyby Ta for RADAR stereogrammetry, a DTM was obtained [*Kirk et al*., 2008, 2009].

[35] Figure 3 shows topography in the Ganesa Macula area. The area appears to be heavily dissected and eroded and, although it is still possible that it was a site of cryovolcanism in the past, there is no clear evidence at present of features that are cryovolcanic in origin. There are lobate deposits adjacent to Ganesa on the east side, and the two most distinct flow features in the area, known collectively as Leilah Fluctus, are two radar-bright flow features farther to the east of Ganesa. These flows are interpreted as fluvial in origin [*Paganelli et al*., 2005; *LeGall et al*., 2010] as they are clearly connected to narrow, sinuous fluvial channels that the topographic data reveal to be deeply incised. Based on these data, our interpretation is that Ganesa Macula and its environs are not cryovolcanic in origin but rather a heavily dissected and eroded region of Titan, with some areas possibly tectonic in origin, particularly those in the western boundary (see Figure 3).

3.2. Sotra Patera Region

[36] A much stronger case for cryovolcanism can be made for the Sotra Patera region, which hosts Titan's highest known mountain (Doom Mons, 40.4°W, 14.7°S) and deepest known pit (Sotra Patera, 40.0°W, 14.5°S) and a well-organized assemblage of other mountains, pits, and flow-like radar-bright lobes. The Sotra Patera region was initially identified

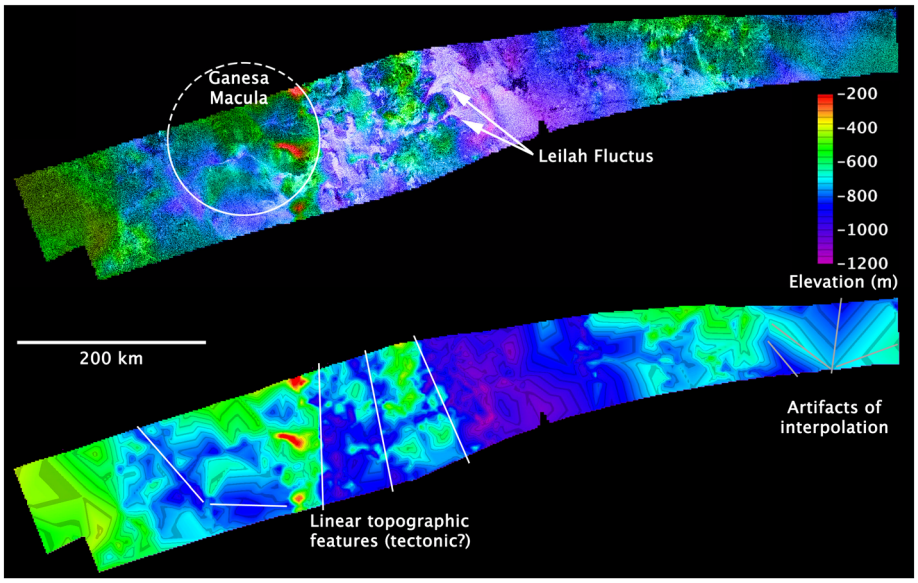

Figure 3. Two views showing results of topographic mapping over the Ganesa Macula region in Equirectangular projection with north at top. Top image shows the SAR image color-coded according to elevation; bottom image shows the color coding without the image. Ganesa (87.3°W, 50.0°N) is the apparently circular feature on the left-hand side of the swath in the upper image. The lower image shows that the northern and eastern parts of Ganesa are elevated relative to the southern and western sides. Flow deposits can be seen in the center of the upper image (Leilah Fluctus; 77.8°W, 50.5°N); they are connected to sinuous fluvial channels. These flow deposits are interpreted as fluvial. Topographic data provide no evidence for a cryovolcanic origin for any features in this area. The DTM (lower image) shows some linear features (minima and steep breaks in elevation, indicated by white lines) mainly around Ganesa itself in the western half of the DTM, suggesting that tectonics played a part in the formation of this feature. However, note that the linear "features" over short distances seen mainly at the east end of the DTM (gray lines) are not real topographic features but artifacts of the mapping process resulting from interpolating a very sparse set of elevation points in this area.

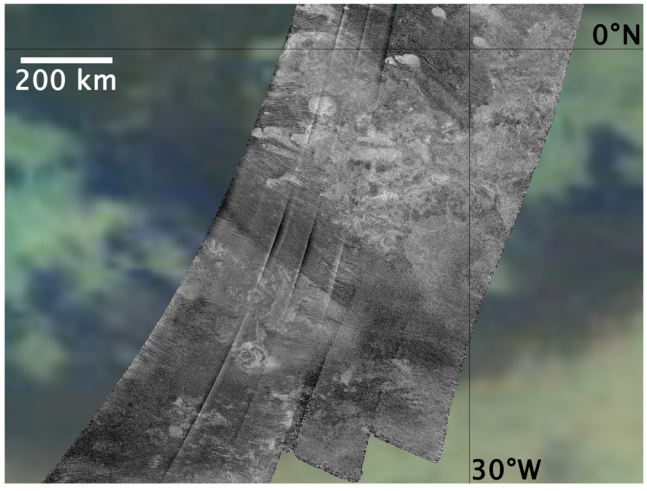

Figure 4. The region formerly known as Sotra Facula (centered at 39.8°W, 12.5°S) was thus named because it appears bright at visible wavelengths. Images from two RADAR SAR swaths, T25 and T28, are superposed on the VIMS global map and show that the region is also bright at radar wavelengths. Dune fields appear as patches of linear, radar-dark features in the middle of the image. See Figure 8 for VIMS data over SAR.

as a bright region at near-infrared wavelengths and was observed in SAR mode in the T25 and T28 flybys (Figure 4). The initial interpretation [*Lopes et al*., 2010a] was of a cryovolcanic edifice consisting of a partial caldera ~30 km in diameter, adjacent to a relatively steep-sided mountain or dome ~40 km across. *Lopes et al*. [2010a] also described a bright-edged lobate unit interpreted as a flow ~180 km long, extending to the north of the edifice.

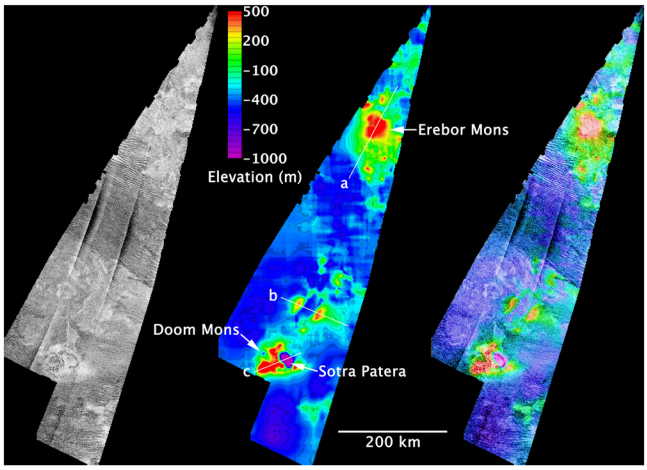

Figure 5. Results of SAR stereo over the Sotra region. The image on the left-hand side is SAR. The central image shows a color-coded DTM; the white lines show where three profiles were obtained from (see Figure 6 for profiles). The SAR and DTM are merged on the right-hand side image.

[37] RADAR stereogrammetry [*Kirk et al.*, 2010] obtained from the crossover flyby swaths T25 and T28 allowed detailed analysis of the whole region. Figure 5 shows the SAR swaths covering the Sotra Patera region, and Figure 6 shows the detailed topography of the area. At the southern end of the region is what appears to be the source region. The detailed topography of the source region is shown in Figure 6c. Doom Mons (which may be a volcanic shield or dome) is ~70 km in diameter and 1.45 ± 0.2 km high. Sotra Patera, the depression adjacent to Doom Mons on the eastern side, which we interpret as a caldera or pit, is 1.7 ± 0.2 km deep and so far the deepest local depression identified on Titan. Sotra Patera is oval rather than circular (therefore unlikely to be of impact origin, see discussion below). On the western side of Doom Mons is an indentation about 500–600 m deep and a small roughly circular depression about 400 m deep, possibly another pit, small caldera, or depression formed by an erosional, explosive, or drainage process.

[38] A distinctive radar and topographic pattern defines what we interpret as flow deposits (collectively named Mohini Fluctus, centered at 38.5°W, 11.8°S), which appear to emerge out of Doom Mons. We suggest that Doom Mons is its likely source; however, it is unclear if it comes out of the larger depression or if it flows down the western side of the mountain where the indentation and smaller depression are. Another lobate unit next to the putative source region is narrow (~20 km) but then widens, possibly reflecting a decrease in slope of the underlying ground topography at the time of flow. Similar morphology may be found on flow fields on Earth [e.g., *Lopes and Kilburn*, 1990].

[39] The lobate features (Mohini Fluctus) lack discernible topography near the source area (Figure 6a) and extend to the north/northeast. They are partially covered by dunes, again indicating that they are thin and did not form an obstacle to the deposition of aeolian material (dunes on Titan are commonly diverted by topographic highs; see *Radebaugh et al.* [2008]). However, the lobate morphology suggests that in most places the dunes are deposited around the flow lobes and only locally overlap them. This relationship suggests that the flow lobes are perhaps tens of meters thick—not

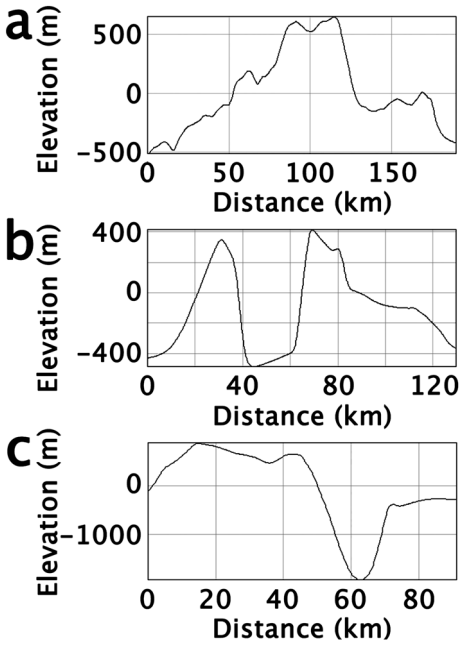

Figure 6. Topographic profiles of features in the Sotra region. Refer to Figure 5 for locations. (a) Topography of the northern region, showing Erebor Mons and surrounding area. Note that the mountain is not apparent from SAR or VIMS data alone, but the DTM shows the feature clearly. (b) Topography of part of the Mohini Fluctus region showing two peaks (possibly from the same original mountain) and an oval depression, possibly remnants of a collapse feature. (c) Topography of the source region. The base level of the region is taken to be −300 m, on the extreme right of the profile line, just NE of the pit. This base elevation is found to be typical of the elevation of the surrounding terrain to the NW and SE of the region. The depth of the Sotra Patera pit from this base level is 1700 m. The highest point on Doom Mons has an elevation 1150 m, which is 1450 m above the chosen base level. The indentation on the NW flank of Doom Mons, not shown on the profile but visible in Figure 5, is about 500 to 600 m deep, and the small pit in this area is about 400 m deep.

enough to be detected clearly in radar topography but enough to partly divert sand dunes whose amplitudes are comparable to flow thickness. The nearest patch of dune material to the source region is located ~20 km away, and the dune band is only ~15 km wide at this location. The flow field is then exposed again and continues between two topographic highs (Figure 6b) that reach ~800 m and appear to channel the flow field. It is possible that these hills form two sides of a ~40 by 70 km oval feature whose middle has collapsed and now forms a depression. Mohini Fluctus extends north/northeast and west until it becomes covered by a swath of dunes, ~200 km from the source area. The swath of dunes is ~180 km wide. The fact that Mohini Fluctus is partially covered by dunes indicates that the dunes are younger, agreeing with the general age relationships identified in *Lopes et al*. [2010a].

[40] To the north of the dune field is a topographically elevated area, which appears mottled in SAR images and is very similar in morphology to the area in western Xanadu identified by *Wall et al*. [2009] and *Nelson et al*. [2009b] as possibly consisting of cryovolcanic flows. This area is elevated above the surrounding dune fields, with a mountain ~40 km in diameter, Erebor Mons (36.2°W, 5.0°S), which stands at an elevation more than 1000 m above the dunes (Figure 6a). This is a good example of a feature not being readily apparent from SAR images (Figure 5) but easily discernible in the topographic data. This northern area around Erebor Mons also shows lobate deposits, which extend to the north/northeast up to another dune field at the very end of the overlapping region between the two SAR swaths, and extends >200 km to the east in the nonstereo image coverage (Figure 4). As in Mohini Fluctus (Figure 6b), little local relief correlated with the bright and dark mottling can be identified in the topographic model here, so the lobate deposits are probably less than 100 m thick.

[41] The three areas in the Sotra Patera region of highest elevations are aligned in a NNE trend, to which the long axis of the middle ovoid is roughly parallel. This may suggest an underlying tectonic control in the region. The depressions in the region are all ovoid rather than circular, indicating that they are unlikely to be of impact origin. The best defined depression is at the southern end (Figure 6c). We have compared the depth-diameter ratio for this depression to those for known impact craters on Ganymede, a moon with similar gravity and crustal composition, from *Schenk* [2002] in Figure 7. Six craters with known depths on Titan are plotted for comparison [*Neish et al*., 2013]. In general, the depths of Titan's craters are within the range of crater depths observed on Ganymede but several hundreds of meters shallower than the average depth for Ganymede craters. In contrast, Sotra Patera is a 18×30 km elliptical depression which is about twice as deep (1.7 ± 0.2 km) and deeper than any known crater on Ganymede [*Bray et al*., 2012], strongly supporting the conclusion that it is not an impact crater.

[42] Data from VIMS are superposed on data from RADAR in Figure 8, showing compositional differences between the dune field (which appears bluish) and the mountains (Doom and Erebor) and Mohini Fluctus, which are part of the equatorial bright spectral unit, as specified in *Barnes et al*. [2007a]. The majority of Titan's tropics belong to this spectral unit, including all of the near-infrared bright material except for Xanadu (which shows a unique and distinct spectral

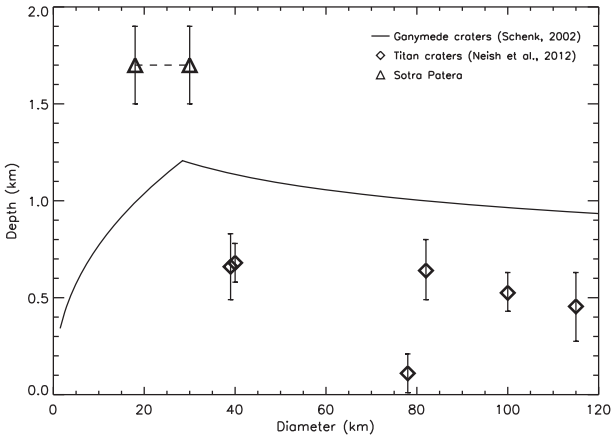

Figure 7. Crater depth for Titan's craters (diamonds) are compared to data from the Sotra Patera ovoid depression (triangles represent the semi-major and semi-minor axes of the ovoid) as well as to the average depth to diameter trend for Ganymede craters determined by *Schenk* [2002].

character). Specifically, the highlands next to the *Huygens* landing site [*Rodriguez et al*., 2006], Tortola Facula [*Sotin et al*., 2005], and the ejecta blankets of Sinlap [*Le Mouelic et al*., 2008] and Selk [*Soderblom et al*., 2010] craters have spectra that match that of Sotra Patera, Erebor and Doom Montes, and Mohini Fluctus regions and also fall into their equatorial bright spectral unit. Analysis by *Soderblom et al*. [2007] indicates that the equatorial bright unit probably does not represent crustal bedrock. Instead, its spectral character implies that it is covered by a relatively thin coating composed of organic atmospheric fallout.

[43] Thus, the spectrum of the Montes and Mohini Fluctus, as measured by VIMS, likely does not constrain the composition of the putative materials. Instead, the existence of this thin coating indicates that these features have been on Titan's surface sufficiently long for a thin coating to be deposited from the atmosphere, probably more than a few tens of thousands of years. This lower limit comes from predicted rates of atmospheric fallout [*Toon et al*., 1980; *Rannou et al*., 2002]. The spectral similarity between the overall Sotra region and Tortola Facula (discussed below) do not necessarily imply similar formation mechanisms or similar bedrock compositions. This likely results from both age and topography, however formed.

[44] Equatorial bright spectral units mapped so far all seem to stand topographically higher than surrounding darker units. While this correlation may not always hold, it is true at the Huygens landing site [*Rodriguez et al*., 2006], Chusuk Planitia [*Jaumann et al*., 2008], and Sinlap [*Le Mouelic et al*., 2008] and Selk [*Soderblom et al*., 2009] craters. The correlation holds at the Sotra Patera and Doom and Erebor Montes region. One hypothesis for the correlation between the equatorial bright spectral unit and relatively high topography is that lower areas have both aeolian and fluvial deposition processes that operate faster than atmospheric fallout, whereas organic haze coating high-altitude areas has no depositional competition or significant erosion [*Barnes et al*., 2007b].

[45] Brightness variations at the Sotra Patera and Doom and Erebor Montes region are consistent with this

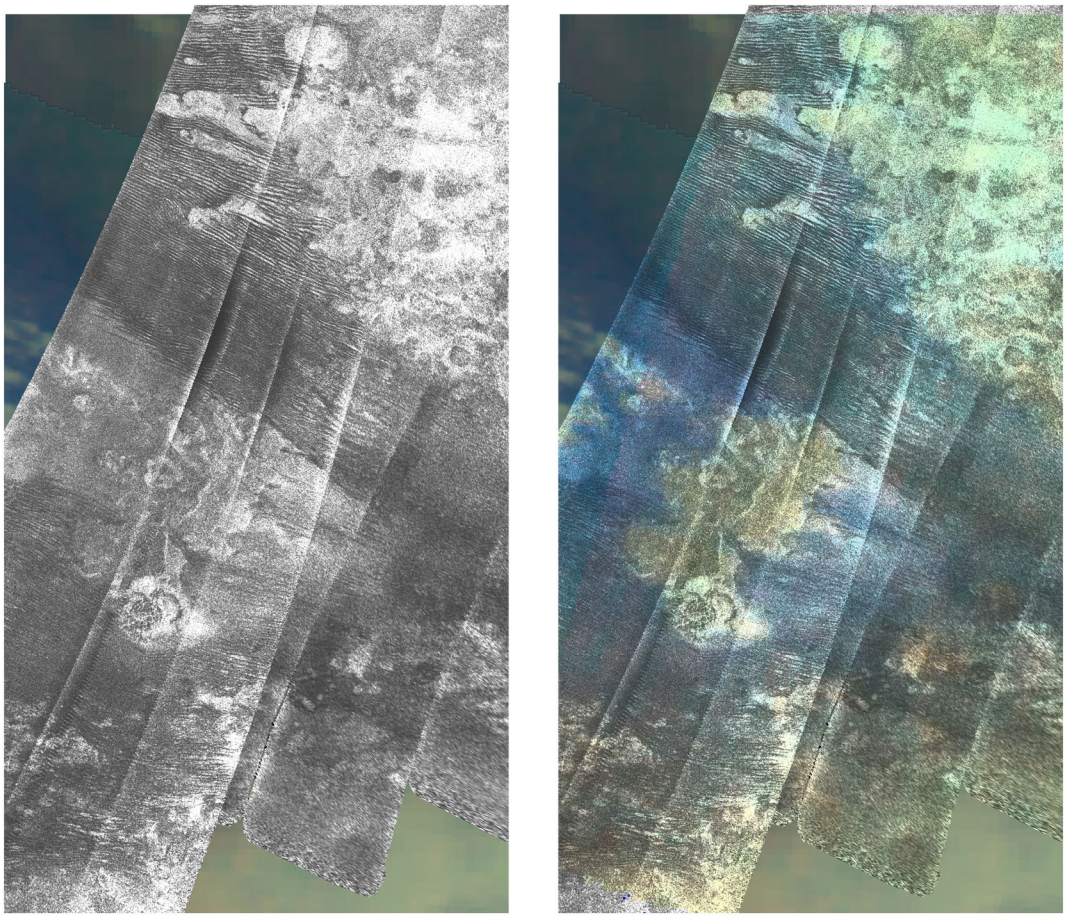

Figure 8. SAR and VIMS data for the Sotra Patera region (images are centered at approximately 38.5°W, 11.8°S). North is at the top. The left-hand side image shows SAR data over VIMS background. The right-hand side image shows VIMS data over SAR showing the dune fields in blue and the candidate cryovolcanic features in shades of green and brown.

hypothesis, too. The reason why the region is readily discernible in near-infrared imaging is that it is surrounded by lower-lying terrain of different spectral signatures. To the north and south of the region, the lowlands are covered in aeolian dune material (described as the Dark Brown spectral unit by *Soderblom et al*. [2007] and *Barnes et al*. [2007a]). East and west of the region are Dark Blue terrains, similar to that at the precise location where Huygens set down. *Rodriguez et al*. [2006] showed that the spectrum of Dark Blue terrain is consistent with a local increase in the fraction of water ice; this material may represent eroded material transported down from neighboring highlands by fluvial processes [*Barnes et al*., 2007b]. Cryovolcanic processes that occur within Titan's highlands might be much harder to identify in near-infrared imaging because they will have lower contrast with their surroundings.

[46] The topography, combined with SAR imaging and VIMS data, strongly suggests that the Sotra Patera, Mohini Fluctus, and Doom and Erebor Montes region is an area of multiple cryovolcanic features: two volcanic mountains (Doom and Erebor Montes), a deep noncircular depression (Sotra Patera) which we interpret to be a collapse feature, a flow (Mohini Fluctus) that appears to emerge from Doom Mons, other noncircular depressions interpreted as collapse features between the two montes, and a series of flows surrounding Erebor Mons. Of particular interest is the fact that the area is totally devoid of fluvial channels, making a fluvial origin for the flows unlikely. Moreover, the dune field that lies between Doom and Erebor Montes indicates that this is a dry region. The fact that the depressions, including Sotra Patera, are not circular makes an impact origin unlikely for these features; furthermore, there is no evidence of any impact ejecta blanket surrounding the depressions. Furthermore, the occurrence of Titan's deepest known depression and several lesser depressions in such close proximity to some of the most substantial mountains on Titan make it unlikely that impacts—so rare elsewhere on Titan—could explain these features. We conclude that Sotra Patera, Doom and Erebor Montes, and Mohini Fluctus were likely formed by cryovolcanic processes.

3.3. Tortola Facula

[47] The first feature on Titan interpreted as having a possible cryovolcanic origin was Tortola Facula, imaged by VIMS at high resolution in October 2004. Tortola Facula (Figure 9) is ~30 km in diameter and located at 143.1°W, 8.8°N. *Sotin et al*. [2005] argued that the feature, which appeared snail-shaped in the VIMS data, was a cryovolcanic dome or thick cryolava flow. Indeed, the feature as seen by VIMS data appeared morphologically similar to high-silica

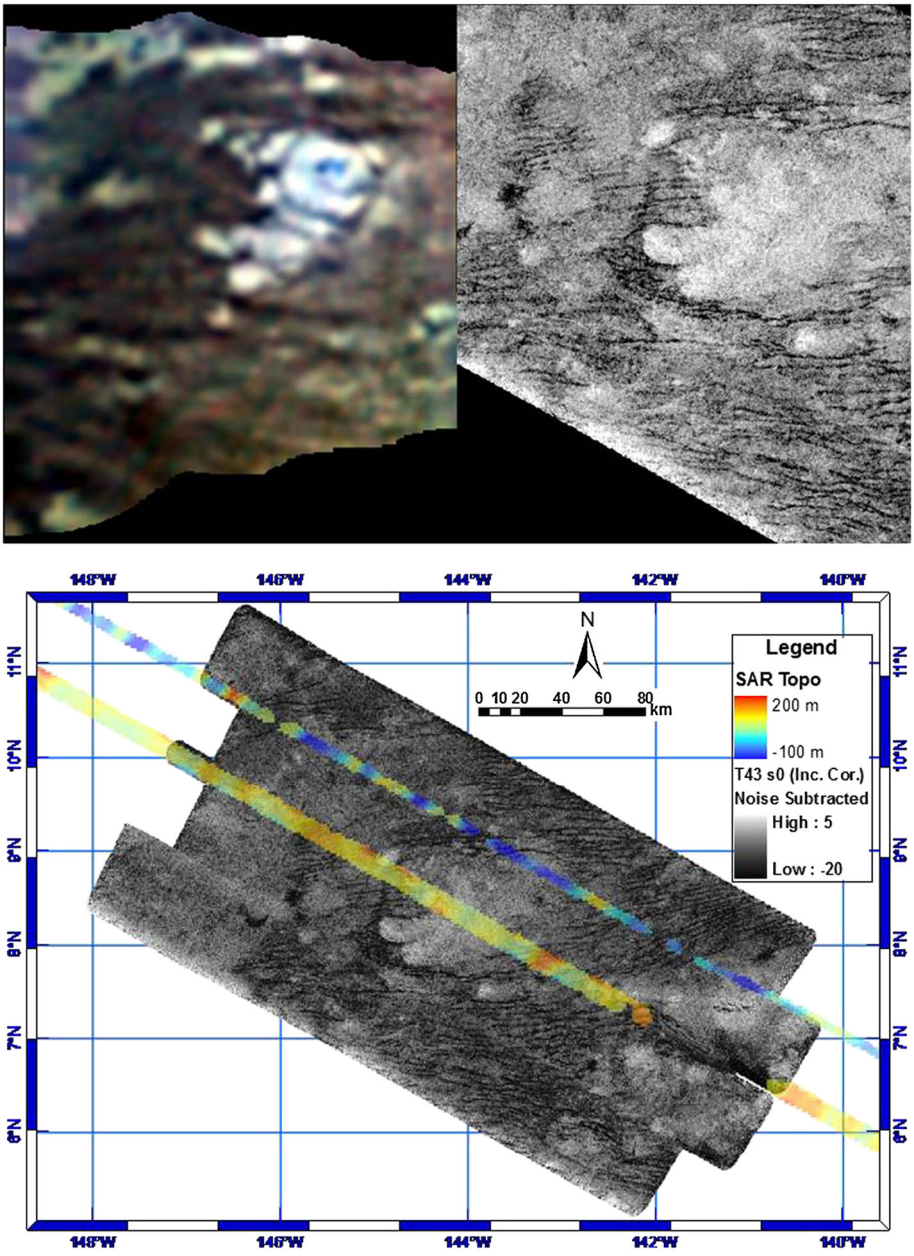

Figure 9. Top: Tortola Facula data from VIMS [after *Sotin et al*., 2005] and RADAR SAR. Tortola Facula (143.1°W, 8.8°N) is the bright, "snail-like" feature on the VIMS image. Below: Topography (from SARTopo method) over the region shows that Tortola Facula is not significantly elevated over the surrounding terrain and dune fields.

lava flows or coulees on Earth, such as the Chao dacite in Chile [*Hayes et al*., 2008a].

[48] SAR data obtained in May 2008 (T43 flyby) did not show evidence that Tortola Facula is cryovolcanic in origin [*Hayes et al*., 2008a; *Moore and Pappalardo*, 2011]. Specifically, the higher resolution imagery failed to reveal features such as flow fronts and festoons that would be diagnostic of a highly viscous flow. Instead, the terrain revealed by SAR at this location (Figure 9) is morphologically similar to terrain observed in many scattered patches on Titan, including Xanadu, which were mapped as hummocky and mountainous terrain by *Lopes et al*. [2010a]. *Hayes et al*. [2008a] find that, from a scattering analysis of the bright terrain in Tortula, this terrain is diffusely scattering, similar to Xanadu terrains, likely consisting of a powdery or rough surface layer that diffusively absorbs and reflects incoming 2 cm radiation. This was also suggested by *Sotin et al*. [2010] from a comparison of the VIMS and SAR images of this area. Although specific details in the radar and optical images correlate well, the shape of the feature looks different, and the "snail-like" brightness pattern seen in the VIMS image is not visible in radar. Therefore, the pattern observed in VIMS data must be distinct either compositionally or in particle size, or both, relative to surrounding terrain.

[49] Topographic data do not support a cryovolcanic origin for Tortola Facula, although the data (from SARTopo)

indicate that the feature is elevated ~100 m relative to the surrounding terrains which contain dune fields. Tortola, however, is not higher than the tops of the dunes. In summary, Tortola Facula is now interpreted as an exposed patch of mountainous and hummocky terrain, similar to many others scattered across Titan.

3.4. Hotei Regio

[50] This candidate cryovolcanic region, centered at ~78°W, 26°S, has been proposed as one of two possibly active areas on Titan [*Nelson et al*., 2009a] on the basis of spectral changes in VIMS data, attributed to changes in the amount of ammonia frost. The existence of these changes has been contested by *Soderblom et al*. [2009]. However, their work also interpreted the region as cryovolcanic, with multiple overlapping flow lobes, and suggested that two large, roughly circular areas apparent in VIMS images could be calderas.

[51] Hotei Regio is unusually bright at 5 µm [*Barnes et al*., 2005], similar to Tui Regio (see next section). SAR images revealed lobate features that form radar-bright and radar-dark patterns. *Wall et al*. [2009] interpreted the radar-bright features as likely cryovolcanic in origin. However, when topographic data obtained from the overlap between SAR swaths (T41 and T43) enabled stereo determination of elevations [*Kirk et al*., 2008; 2009], results revealed topographically high lobate areas, with heights of ~200 m (Figures 10a and 10b) above the base level at which the channels are found. This is more consistent with a cryovolcanic than fluvial origin, as it implies a complex rheology, such as might be expected for ammonia-water-methanol mixtures [*Kargel et al*., 1991; see also analysis in *Lopes et al*., 2007].

[52] *Moore and Howard* [2010] argued that the radar-bright, topographically low regions in both Hotei and Tui Regios are clusters of paleolakes, similar to those seen at high latitudes in the SAR data. *Moore and Pappalardo* [2011] argued that the presence of many radar-bright valleys, likely fluvial in origin, running onto the radar-bright materials suggest that these bright materials result from fluvial erosion and downcutting of channels, as observed in sediment-filled valleys on Earth. This interpretation disagrees with that of *Soderblom et al*. [2009], who suggested that the deposits associated with the fluvial channels are limited to small basal VIMS "Dark Blue" units around the edges of the thick lobate features.

[53] *Barnes et al*. [2011] argued that the similarities between spectra of the dry lakebeds at Titan's poles, interpreted as evaporitic deposits, and the 5 µm-bright Tui and Hotei Regios, although not definitive, allows for the possibility of a common origin. However, *Barnes et al*. [2011] pointed out that since the radar-dark, lobate deposits seen in SAR images do not show the spectral signature of evaporites, they are not inconsistent with a cryovolcanic origin.

[54] Given the presence of channels associated with mountainous terrains, there is no question that fluvial processes have operated in the Hotei Regio area. *Barnes et al*. [2011] suggest that Hotei is a dry lakebed that has been filled with liquid in geologically recent times but point out that cryovolcanism could have taken place as well. However, we argue that the thickness of the flows points to cryovolcanism as the most likely origin of these features. Figure 10b shows a topographic profile across one of the radar-dark flows showing it to be ~200 m high. The thicker parts of the flows are as high as the nearer parts of the mountains out of which the fluvial channels emanate. The tops of the flows are substantially higher than these fluvial channels. Topography also shows that there is no discernible elevation change along the channels (between head and mouth of channels), but the flows are 100 to 200 m higher in elevation than the channels. It seems unlikely that the channels we see today could account for the formation of these thick flows. It is possible that the topographically

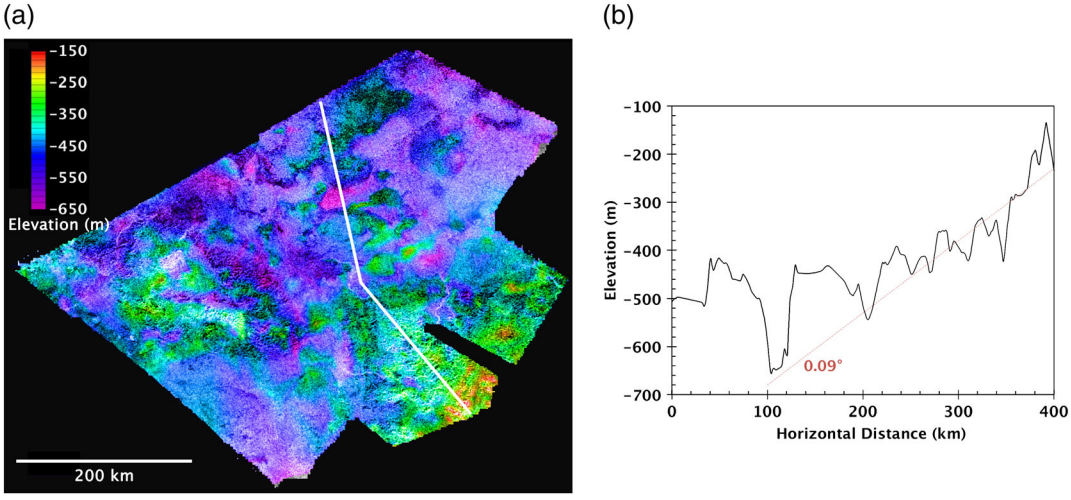

Figure 10. (a) Perspective view of the Hotei Regio area from a DTM, with a vertical exaggeration of 40. The white line indicates the location of the profile in Figure 10b. On the right-hand side are the mountains forming Hotei Arcus, and a few channels are seen coming down from the mountains. High areas thought to be flows are shown in green (see profile in Figure 10b) and are about 200 m high. Low intraflow areas are shown in purple. There is no clear connection between the channels and putative flows, and the inferred flow adjacent to a channel is topographically higher than the channel. (b) Elevation profile of Hotei Regio area from a DTM. See Figure 10a for location of profile. Putative flows are about 200 m high.

low, radar-bright areas may be paleolakes as suggested by *Moore and Howard* [2010], but this does not conflict with the interpretation that the radar-dark, topographically high areas were formed by cryovolcanism.

[55] Backscatter analysis of the putative cryovolcanic terrains on Titan, mostly based on Hotei Regio and Tui Regio, indicate a surface that is distinct from other Titan terrains [*Wye*, 2011]. Most notably, these surfaces have a very large diffuse exponent (a value of the cosine power law exponent approaching 3), indicating the presence of a very focused diffuse scattering mechanism that is not very efficient at large incidence angles. Indeed, the diffuse component falls off much more steeply with incidence angle than is otherwise common on Titan (Figure 11). Furthermore, the measured diffuse echo is only 70% of the total echo power, in contrast to the >82% diffuse fractions observed elsewhere [*Wye*, 2011]. The diffuse scattering behavior described by *Wye* [2011] suggests that volume scattering is not as prevalent in these putative cryovolcanic terrains, either because the medium is more radar-absorptive or an insufficient number of scattering centers exist in the volume. It is also possible that the diffuse scattering mechanism is different altogether. In addition to exhibiting unique diffuse scattering behavior, these putative cryovolcanic terrains suggest a higher dielectric constant than any other terrain on Titan observed and modeled with RADAR. Composite backscatter model results indicate a dielectric constant greater than 3.5, a dielectric constant that is consistent with (although does not prove) the presence of ammonia-water ice [*Wye*, 2011]. If ammonia is a component of the cryovolcanic material, this may also explain the poorer diffuse scattering levels, as the higher absorptive properties of water-ammonia ice reduce the strength of the radar echo within the volume of the material. For example, *Ostro et al.* [2006] noted how the hemispheric asymmetry of Iapetus lessens with increasing wavelength, suggesting a possible increase in contamination with depth, and offered ammonia as a candidate for this contamination due to its absorptive properties.

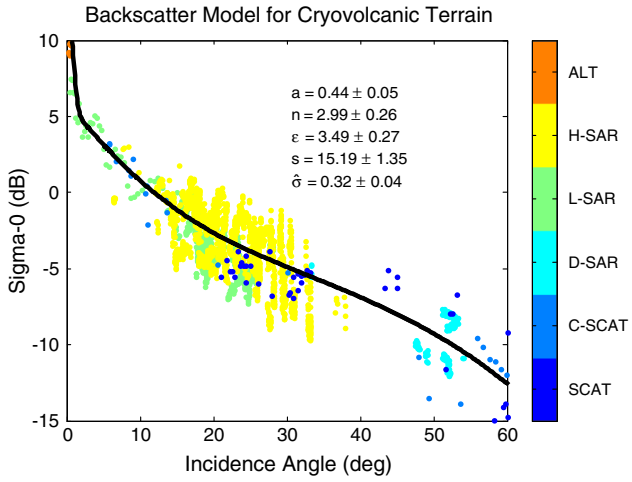

Figure 11. The backscatter model that best describes the mapped cryovolcanic terrain is a composite model that consists of the sum of Gaussian and exponential quasi-specular models and a diffuse model, as described in *Wye* [2011]. The parameters of the composite model suggest a surface with a dielectric constant less than 3.49, an rms surface slope near 15°, a diffuse amplitude of 0.44, and a diffuse power of 2.99. The total radar albedo (in the same-sense linear polarization) is 0.32. The cross-section data points are colored by their radar mode and show that the collective set of data is well calibrated to the same scale.

[56] In summary, we conclude that cryovolcanism is a likely origin for the radar-dark flows in Hotei Regio, although other features in the region could have been formed by fluvial or lacustrine processes.

3.5. Tui Regio

[57] The western part of Tui Regio (~125°W, 24°S) is a large ($>3 \times 10^4$ km^2) region that is bright at 5 μm [*Barnes et al.*, 2006]. Numerous lobate deposits are apparent in VIMS data, and *Barnes et al.* [2006] interpreted it as a field of cryovolcanic flows. These lobate deposits are also apparent in SAR data [*Stofan et al.*, 2009]. There are morphological similarities between Tui and Hotei that are apparent in SAR data: bright and dark lobate features (although not as well defined as in Hotei), fluvial channels, and nearby mountains.

[58] Although multiple RADAR images of Tui Regio have some overlap, they have relatively low resolution and have not been analyzed stereogrammetrically. We have therefore obtained limited topographic information using the SARTopo technique (Figure 12). There is no correlation between lobate deposits (which here appear radar-bright) and higher elevations; in fact, the lobate deposits appear to be depressions. However, we caution that the SARTopo data for Tui are of relatively low quality given that Tui is located at the end of the swath, where the signal-to-noise ratio is poor.

[59] The topographic results do not support a cryovolcanic origin for the lobate features but, given the limited extent and relatively low quality of the data—in particular, the difficulty of interpreting complex three-dimensional structures from elevation profiles—we hesitate to form definite conclusions. Backscatter analysis by *Wye* [2011], as discussed above, suggests that Tui and Hotei are similar terrains, possibly having ammonia as a component, and these regions differ from other terrains on Titan. These anomalous backscatter results are consistent with but do not uniquely support a cryovolcanic origin. Other recent results suggest that Tui is likely a lacustrine environment. *Moore and Howard* [2010] argue that the features in Tui are clusters of paleolakes. *Barnes et al.* [2011] support the interpretation that the Tui Region area has evaporitic deposits, indicating fluvial deposition has also been important in this region, although this does not rule out that cryovolcanism took place as well. Clearly, Tui is distinct from most other terrains on Titan, but its origin is still somewhat unclear, so we classify it as "possibly cryovolcanic."

3.6. Winia Fluctus

[60] This large radar-bright region centered at ~30°W, 45°W (Figure 13), first seen in the SAR data from Cassini's Ta flyby, was interpreted as a likely cryovolcanic flow field by *Elachi et al.* [2005] and *Lopes et al.* [2007], although a fluvial origin was also considered possible. Data from the T23 flyby showed that the extent of the putative flow field was larger than 90,000 km^2 [*Lopes et al.*,

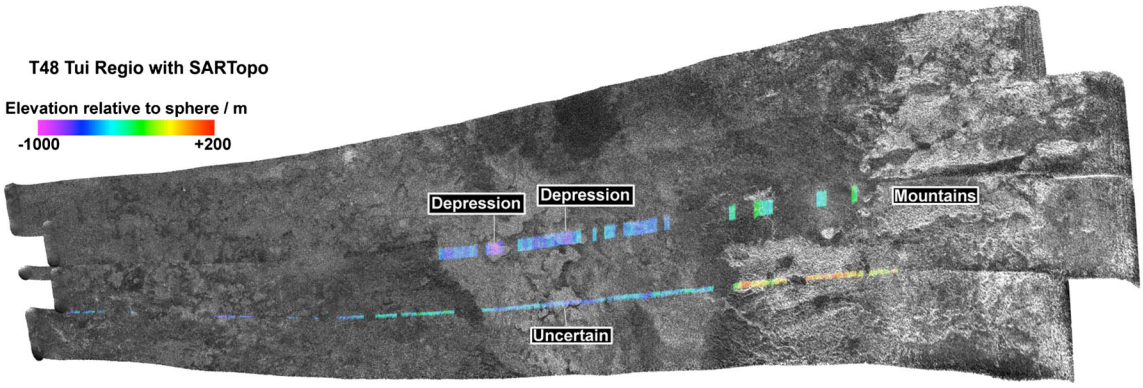

Figure 12. SARTopo data over Tui Regio (~125°W, 24°S) from T48 data. North is at the top. SARTopo tracks near the end of the T48 swath are limited due to poor signal-to-noise ratio, but show what appears to be an inconsistent correlation between RADAR bright patches and elevation. Radar-bright mountains to the east (right-hand side) are topographically high as expected. However, radar-bright features initially interpreted as flows appear to be, in most cases, depressions consistent with lakebeds [*Mitchell and Malaska*, 2011], similar to those seen in the north polar region [*Hayes et al*., 2008b].

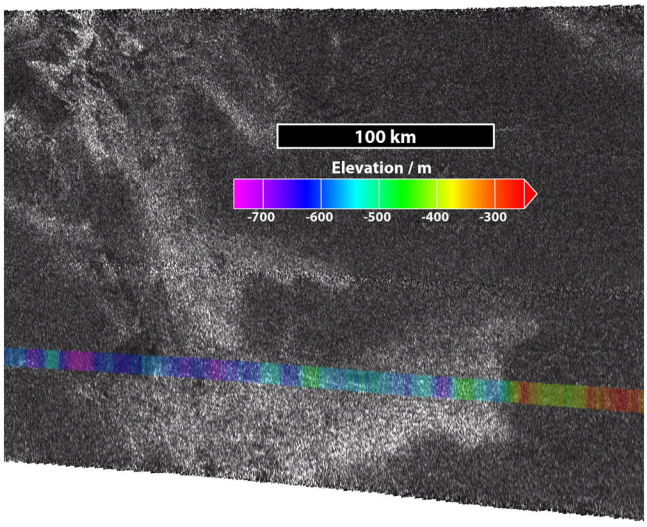

Figure 13. Winia Fluctus: SARTopo tracks show that apparent radar-bright lobate flows at Winia Fluctus are topographically negative, rather than positive. On the basis of topography, we favor an origin as a fluvially carved valley system.

2010a], the largest of its type on Titan. Winia Fluctus consists of a series of lobate bright deposits that all appear to flow towards the south and east. This is consistent with the direction of the nearby Rohe Fluctus and also the slope of the altimetry track obtained east-southeast of the Ta swath [*Kirk et al*., 2005].

[61] Data from SARTopo are, however, not consistent with the interpretation of these apparent lobate features being flow deposits, whether cryovolcanic or fluvial. Figure 13 shows the SARTopo data superposed on the SAR image from the Ta flyby. Specifically, the features interpreted to be lobate flow deposits appear to be depressed features. In addition, dune-like features observed on the floors of Winia in the T23 scene are difficult to account for on top of lava flows. Dunes at high local topographic elevations are rare [*LeGall et al*., 2012], but it is conceivable that a valley-like morphology would focus winds, creating local conditions suitable for dune formation. Based on these new data, our current interpretation of Winia Fluctus is that it is likely a fluvially carved valley system.

3.7. Western Xanadu Region

[62] Candidate cryovolcanic flows are seen in SAR data on the western part of Xanadu (centered at ~140°W, 10°S), coinciding with a region that *Nelson et al*. [2009b] reported had photometric changes similar to those of Hotei Regio. *Wall et al*. [2009] noted the morphological similarity in the SAR data between Hotei and Western Xanadu, interpreting these as regions of overlapping cryovolcanic flows. Although no new SAR data are available for Western Xanadu since the study of *Wall et al*. [2009], we note here the morphological

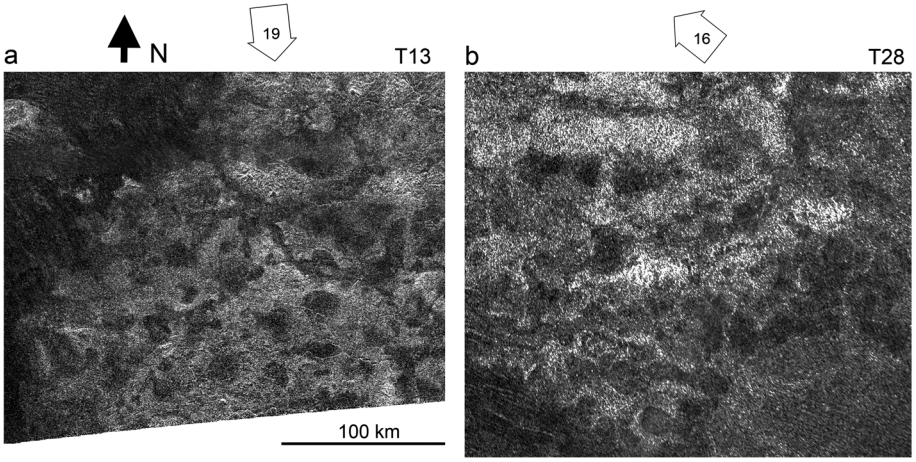

Figure 14. Western Xanadu (left, image centered at 146°W, 12°S) comparison with the Erebor Mons region (right, image centered at 33.3°W, 7.0°S). Open arrows indicate SAR illumination direction and incidence angle. Western Xanadu was interpreted as a region containing cryovolcanic flows by *Wall et al*. [2009]. Both Western Xanadu and the Erebor Mons region show a pattern of lobate features that appear to be overlapping flows. Topographic data (Figure 6) revealed the existence of Erebor Mons (in the upper right of the SAR image on right) and strengthened the cryovolcanic interpretation for the region. The available topographic data (SARTopo) for Western Xanadu are too sparse to be diagnostic.

similarity between the Western Xanadu area and the north Erebor Mons area, as displayed in Figure 14. These regions show a pattern of lobate features that appear to be overlapping flows. With the aid of topographic data, we interpreted the northern Sotra region as a likely cryovolcanic region (see section 3.2). Topographic data for the Western Xanadu region are too sparse to be diagnostic, and VIMS data are of insufficient resolution, but on the basis of the morphological similarity in SAR data to those of both northern Sotra and Hotei, we classify this region as possibly cryovolcanic.

3.8. Other Candidate Features

[63] Candidate cryovolcanic features on Titan other than the ones above were discussed by *Lopes et al*. [2007]. Considering new mapping efforts and examination of a larger data set, features associated with Ganesa Macula and Winia Fluctus are unlikely to be cryovolcanic. We consider three of the features discussed by *Lopes et al*. [2007, 2010a] to be candidate cryovolcanic features: a flow-like feature in the T3 SAR swath (~70°W, 20°N), a depression and adjacent flow named Rohe Fluctus (37.8°W, 47.3°N), and a noncircular depression which may contain a flow, Ara Fluctus (118.4°W, 39.8°N). VIMS data are available for the flow-like feature in T3, and this was discussed by *Le Corre et al*. [2009], who found compositional differences between the flow and the surrounding terrain and agreed with the cryovolcanic interpretation for this feature. No high-resolution VIMS data are currently available for the other features. SARTopo or new SAR data are also not available for these features except for the flow-like feature in T3. However, the SARTopo data for this feature are too sparse to be diagnostic, although it is consistent with the

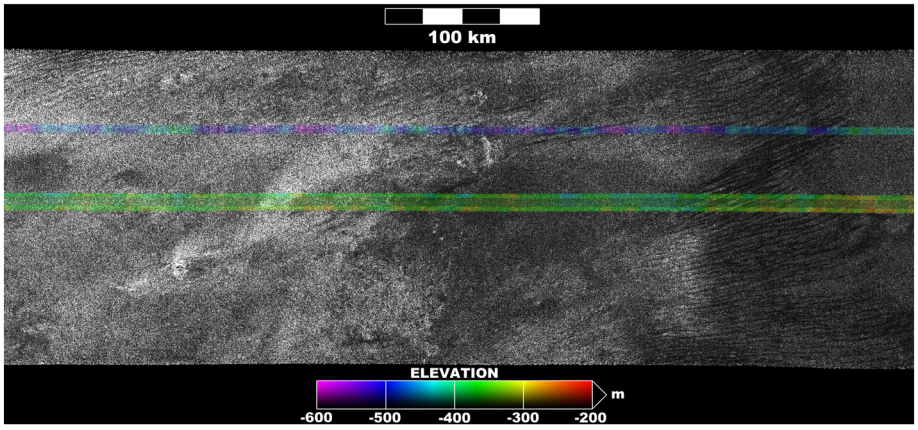

Figure 15. Flow-like feature (~70°W, 47°N) seen in T3 data and interpreted as cryovolcanic by *Lopes et al*. [2007] from radar data and by *Le Corre et al*. [2009] from VIMS data. Although the SARTopo data shown here are too sparse to be diagnostic, it is consistent with a feature flowing downhill.

Table 1. Candidate Cryovolcanic Features on Titan Discussed in This Paper, Center Latitude and Longitude of Feature or Area, and Interpretation

Not Cryovolcanic	Possibly Cryovolcanic	Strongest Candidates
Ganesa Macula (87.3°W, 50.0°N) and associated flow features	Ara Fluctus (118.4°W, 39.8°N)	Sotra Patera (40.0°W, 14.5°S) Doom Mons (40.4°W, 14.7°S) Mohini Fluctus (38.5°W, 11.8°S) Erebor Mons (36.2°W, 5.0°S)
Tortola Facula (143.1°W, 8.8°N)	Western Xanadu flows (~140°W, 10°S)	Hotei Regio flows (~78°W, 26°S)
Winia Fluctus and associated flow features (~30°W, 45°N)	Rohe Fluctus (37.8°W, 47.3°N) "T3" flow (~70°W, 20°N) Tui Regio flows (~125°W, 24°S)	

feature flowing downhill (Figure 15). All the mentioned features are too small in areal extent to be distinguished in radiometry or scatterometry data. In the absence of new data, we keep the interpretation of these features as possibly cryovolcanic.

[64] While the majority of Titan's polar depressions are noncircular and have been associated with dissolution-based formation mechanisms [e.g., *Hayes et al*. 2008b, 2011], some of the more circular depressions have been associated with flow-like features surrounding bright deposits that, in some cases, contain lakes in their floors [*Wood*, 2011]. Although other origins have been suggested for these circular features, *Wood* [2011] argues that the interpretation as volcanic calderas or maars is most consistent with the morphological evidence.

4. Conclusions

4.1. Summary of Results

[65] We have reexamined candidate cryovolcanic features in light of new data, particularly topographic data from both radargrammetry and SARTopo. We have found that topographic data derived from RADAR are invaluable for geologic interpretation of features on Titan. Unlike most other solid bodies in the solar system examined by spacecraft, Titan's haze generally prevents the derivation of topographic data from imaging data. In addition, geologic interpretation of features is hindered by the limitations of the currently available data, particularly spatial resolution.

[66] In previous studies, SAR and VIMS data were used to identify the features named in Table 1, all of which could reasonably be interpreted as cryovolcanic in origin on the basis of those data. However, new information, particularly topographic data, has provided the key to differentiate between the "not cryovolcanic" and "strongest candidates" categories in the table. Ganesa was classified as not cryovolcanic on the basis of radargrammetry that provided a DTM over the region. For Tortola Facula, a combination of SAR and SARTopo data also showed the cryovolcanic interpretation to be unlikely. Although the SARTopo data for Winia Fluctus are limited in areal extent, they were sufficient in this case to show that the feature is not a flow as previously thought.

[67] Most of the "possibly cryovolcanic" features are those for which no new data, particularly no topographic data, are available, and interpretations are made on the basis of morphology from SAR. In the case of Tui Regio, new SARTopo data, VIMS interpretations [*Barnes et al*., 2011], and scatterometry results are not yet sufficient to make a definite interpretation, but the case for a cryovolcanic origin is weak.

[68] Topographic data, and DTMs from stereogrammetry in particular, have revealed that two candidate cryovolcanic regions, Hotei Regio and the region of Sotra Patera, Mohini Fluctus, and Doom and Erebor Montes, are indeed likely to have been formed by cryovolcanism. Hotei Regio had been interpreted as an area of cryovolcanic flows [*Wall et al*., 2009; *Soderblom et al*., 2009] and even the site of possible activity or degassing [*Nelson et al*., 2009a, 2009b]. *Moore and Pappalardo* [2011] argue that the flow-like features were likely depositional features associated with fluvial channels. Topographic results show that the tops of the flow deposits are substantially higher than the fluvial channels, and therefore that interpretation is unlikely. Also, flow deposits are thick (~200 m), a characteristic more consistent with the complex rheology of cryovolcanic flows than sedimentary deposits. Our conclusion is that the Hotei flows are more likely cryovolcanic than fluvial in origin.

[69] We find the Sotra Patera region to host the most compelling candidate cryovolcanic features on Titan on the basis of the combination of SAR imaging, VIMS data, and, in particular, topographic data from RADAR stereogrammetry. We interpret the region as a complex of multiple cryovolcanic features dominated by two mountains, Doom Mons and Erebor Mons. The southernmost mountain, Doom Mons, is adjacent to Sotra Patera, a noncircular pit that is, to date, topographically the deepest known local depression on Titan. We note that the northernmost mountain, Erebor Mons, was not apparent in SAR data and was only discovered in the topographic data. Although topographic data have proven to be a key factor in this study, the findings are limited by the available resolution. Features with subtle topographic differences, such as deposits from highly fluid volcanic flows, would be particularly difficult to distinguish from features of fluvial or mass wasting origins, so the interpretation of flow-like features relies on the geologic context. In this whole region, no fluvial channels or mass wasting scars are seen, making these modes of origin unlikely for the flow deposits.

[70] Due to the small number of features in Table 1 considered to be either strong candidates for cryovolcanism or possible candidates, it is not possible to come to conclusions about their distribution on the surface, but we note that all are located between 30°W–150°W and 30°S–60°N. The northern high latitudes of Titan have multiple caldera-like features [*Wood*, 2011], but these are not discussed in this paper as no relevant topographic data or VIMS data are available for them. Of the candidate features in Table 1,

we note that four are located near the edges of Xanadu [*Lopes et al*., 2010a, 2010b]. It has been suggested that faulting along the boundaries of Xanadu may have provided conduits for magmas to reach the surface [*Radebaugh et al*., 2010].

[71] The likely existence of different types of volcanic landforms—tall mountains, a large caldera-like depression, lengthy flows, and other possibly collapse features—implies that Titan has experienced a variety of types of volcanism in different locations. It is quite possible that many other volcanic landforms occur but that erosion has weakened their morphologic signatures or that Cassini data are either not available or of insufficient resolution for identification of features to be possible.

4.2. Implications

[72] The data presented in this paper indicate that cryovolcanism likely happened on Titan, but, as previous studies show [e.g., *Lopes et al*., 2010a, 2010b], it is not the dominant resurfacing process, with exogenic processes (aeolian, fluvial, and atmospheric deposition) accounting for most of the observed surface geology. If cryovolcanism occurred on Titan and was responsible for the formation of features such as the flows at Hotei and the flows of Mohini Fluctus, deep pit (Sotra Patera), and mountains (Doom and Erebor Montes), what are the implications for eruption style and composition?

[73] The fact that aqueous cryomagmas are negatively buoyant makes the use of ascent models based on terrestrial (and silicate) models problematic, in particular those that involve formation of a diapir or mantle plume at the base of the icy shell, but several studies have proposed ways to overcome the cryomagma ascent problem. One mechanism calls for inducing positive buoyancy through exsolution of volatiles following decompression, and the subsequent ascent along fluid-filled fractures (analogous to dykes) from the base of the ice shell [*Crawford and Stevenson*, 1988; *Lorenz*, 1996], or explosive eruption of sprays [*Fagents et al*., 2000]. Effusive eruptions have been hypothesized to occur by pressurization of discrete liquid chambers [*Fagents*, 2003; *Showman et al*., 2004] or an entire ocean during freezing and volume changes [*Manga and Wang*, 2007]. *Mitri and Showman* [2008] and *Tobie et al*. [2008] argue that partial melting of the ice shell by tidal dissipation facilitates the formation of near-surface reservoirs without buoyancy requirements. After Voyager observations of Triton, *Croft et al*. [1988] proposed that denser silicate material could be incorporated in the ice shell due to incomplete differentiation of meteoritic infall, and this rock component might have a large enough effect on the crustal density to make melt buoyancy possible. Some cryolavas may have the low densities needed to ascend through a water-ice-dominated crust. Lastly, solid-state convection in the ice shell can advect heat and possibly chemicals upward and mobilize near-surface pockets of salt- or ammonia-rich ices [*Head and Pappalardo*, 1999; *Mitri et al*., 2008; *Choukroun et al*., 2010]. While it is beyond the scope of this paper to try to distinguish among these models, we note that these studies argue that, theoretically at least, cryovolcanism is possible on icy satellites including Titan.

[74] The composition of cryomagma is an important factor not only in terms of the ascent mechanism but also for the landforms that can result. The basic interpretation that cryovolcanism produced or contributed to the observed landforms does not in itself provide any tight constraint on composition. It is reasonable to assume that the cryovolcanic substance is a mobile material able to exist as a liquid in the subsurface, to rise buoyantly to the surface, and then to solidify on the surface. In principle, cryomagmas may be composed of liquids plus solids and gases, and the combination is what must be less dense than the average crustal density from the partial melting zone to the surface.

[75] Aqueous cryolavas make up one class of potential eruptive materials, because ice is known to be a major mineral constituent of the surfaces, crusts, and interiors of icy satellites, and Titan should be no exception. Partial melting of ice admixed with other materials produces aqueous solutions. Other substances known to be present on Titan and other icy moons can melt at temperatures lower than the range over which ice can melt, and some of these could be more likely to occur if interior temperatures are very low due either to a low energy budget or due to low-temperature solid-state convection [e.g., *Mitri and Showman*, 2008; *Choukroun et al*., 2010]. We may consider the collective suite of materials identified to date in the Saturn system as a list of possible solvents or solutes. This list of candidate materials includes H_2O, NH_3, CO_2, methanol, and a variety of other hydrocarbon and organic substances. Even the two primary constituents of Titan's atmosphere, CH_4 and N_2, could exist as dissolved solutes, an exsolving gas phase, or guest species in clathrates comprising part of the frozen cryolavas. Ethane and propane (surface liquids) as well as acetylene (a possible surface material) can also participate in clathrate formation [*Consani and Pimentel*, 1987; *Kirchner et al*., 2004]. Water as a solvent may be expected to contain polar molecular solutes, such as methanol or ammonia, or ionically bonded salts. If ammonia is present in aqueous solution, ammonium salts are also possible [*Kargel*, 1992; *Marion et al*., 2012].

[76] While the morphology of the putative cryovolcanic features does not place hard constraints on specific compositions, materials forming thick flows such as those at Hotei either (1) are not brines (which have low viscosities when totally liquid) and are instead flows of ammonia-water-ice slurries [*Kargel et al*., 1991] or ammonia-water-methanol as proposed for Rohe Fluctus [*Lopes et al*., 2007]; or (2) are brines but flowed with large amounts of suspended ice and so behaved like brine-ice slurry flows.

[77] The scale and morphology of the Sotra Patera complex, in particular the size of Doom and Erebor Montes and the deep pit, Sotra Patera, are more consistent with large-scale processes rather than a local heat source remelting materials such as hydrocarbons. Sotra Patera's pit morphologically resembles calderas and other volcanic pits such as maars and pit craters, but it is very deep. Possible explanations for Sotra Patera and its great depth include collapse due to removal of material from the subsurface by either explosive or effusive eruptions, with either case implying the presence of a voluminous magma chamber and possibly vesiculating cryolavas in the upper ice shell. On Titan, the presence of a thick 1.5 bar atmosphere (0.15 MPa) may act to suppress explosive eruptions, relative to effusive volcanism [*Lorenz*, 1996], but high vesicular porosity and low magma density is possible; thus, Strombolian-type explosive activity could occur.

[78] It is difficult to account for the existence of a voluminous magma chamber, the presence of which in nonplate tectonic silicate rock settings is the result of mantle plumes rising buoyantly in the crust and stalling. However, unlike on rocky worlds, where unvesiculated liquid magma tends to be less dense than heavily compacted country rock, any cryomagmas on Titan are likely to be composed primarily of water, which has the opposite density relation. Although nonwater components may be less dense, we have not identified any plausible compositions that would be sufficiently positively buoyant in an ice-rich crust. Even peritectic ammonia hydrates, as proposed by *Kargel et al*., [1991], have a density in excess of that of Ice-I. However, neutral buoyancy and massive intracrustal intrusion [*Head and Wilson*, 1992] by ammonia-water cryomagmas might be readily achieved with just a few percent vesicles [*Croft et al*., 1988] if there were a way to supersaturate the cryomagma at source.

[79] An alternative to water-rich cryomagmas are crust-derived melts, making activity akin to mud volcanism or geysers on Earth. A local source of methane clathrates undergoing heating or depressurization could result in destabilization of trapped volatiles, resulting in a type of volcanism, most likely explosive [*Prockter*, 2004]. Further work on the physical properties of various candidate materials is needed before these possibilities can be assessed.

[80] Caldera-like features—"smooth-floored, walled depressions"—are also seen on Neptune's moon Triton, but they are very different from Sotra Patera in that Triton's are relatively shallow and very wide. However, Triton has many other landforms that resemble terrestrial volcanic features—pitted cones and pit paterae—and have been interpreted as cryovolcanic [*Croft et al*., 1995], and some of these, including a chain of depressions arranged along a rift, are quite similar to but smaller than Sotra Patera. Another type of landform on Triton is the pitted cone. Pitted cones are roughly conical hills with summit pits. It is interesting that these pits often breach one side of the cones, like many terrestrial cinder cones. Sotra Patera on Titan breaches one side of the main edifice (Doom Mons), although in terms of scale Sotra Patera is much larger than the Triton features, where the pits are typically 4 to 7 km in diameter. The pit feature on Triton that is closest in dimensions to Sotra Patera is Kibu, which is ~10 × 15 km in extent and ~500 m deep or less. In comparison, Sotra Patera is 18 × 30 km and 1700 m deep, making it significantly larger than the most prominent pit patera known on Triton and deeper than any on Earth. Also, Triton does not have any topographically high features that are comparable to Doom or Erebor Montes; linear ridges about 300 m high are the most prominent topographically positive features on Triton. It is possible that differences in scales of magmatism and atmospheric pressure could account for the differences, but the key point to note is that both Titan and Triton, icy moons where cryovolcanism may have taken place, have pit features that may be cryovolcanic in origin. Explaining the formation of these pits remains problematic in terms of magma ascent, but it is possible that the same processes apply to both bodies.

[81] The features in the Sotra Patera region (Sotra Patera, Mohini Fluctus, Doom and Erebor Montes) and the thick flows at Hotei Regio are the most compelling cryovolcanic landforms revealed so far by Cassini data, providing evidence that cryovolcanism has played a role in Titan's geologic history and at least a limited role in its methane cycle. It is clear, however, that if the style of cryovolcanism in the Sotra Patera region was a major contributor to Titan's resurfacing and relatively young age, edifices like Doom and Erebor montes should be much more common on Titan's surface than has been observed. If cryovolcanism played an important role in Titan resurfacing, the paucity of features similar to the montes and the patera points to another style of volcanism being far more common, possibly effusive volcanism forming thin flows that may have been partly buried or totally buried by the accumulation of photolysis products created in the upper atmosphere or wind-blown materials.

[82] The "smoking gun" for active cryovolcanism on Titan, in the form of an enhanced thermal signature, active plumes, or surface changes, has not yet been detected. Given that features interpreted as cryovolcanic do not appear to be young, it is possible that cryovolcanism is no longer taking place on Titan. In this case, greater coverage of the surface by Cassini and interpretation of geologic features using several data sets as presented in this paper will provide us the best opportunity to delve into Titan's possible cryovolcanic past.

[83] **Acknowledgments.** Part of this work was carried out at the Jet Propulsion Laboratory, California Institute of Technology, under contract with the National Aeronautics and Space Administration (NASA). We thank Sarah Fagents, Lazlo Kestay, and an anonymous reviewer for comments that greatly improved the manuscript. We also thank the Cassini-Huygens team for the design, development, and operation of the mission. The Cassini-Huygens mission is a joint endeavor of NASA, the European Space Agency (ESA), and the Italian Space Agency (ASI) and is managed by JPL/Caltech under a contract with NASA.

References

Barnes, J. W., et al. (2005), A 5-micron-bright spot on Titan: Evidence for surface diversity, *Science*, *310*, 92–95, doi:10.1126/science.1117075.

Barnes, J. W., et al. (2006), Cassini observations of flow-like features in western Tui Regio, Titan, *Geophys. Res. Lett.*, *33*, L16204, doi:10.1002/2006GL026843.

Barnes, J. W., R. H. Brown, L. Soderblom, B. J. Buratti, C. Sotin, S. Rodriguez, S. Le Mouelic, K. H. Baines, R. Clark, and P. Nicholson (2007a), Global-scale surface spectral variations on Titan seen from Cassini/VIMS, *Icarus*, *186*, 242–258.

Barnes, J. W., et al. (2007b), Near-infrared spectral mapping of Titan's mountains and channels, *J. Geophys. Res.*, *112*, E11006, doi:10.1029/2007JE002932.

Barnes, J. W., et al. (2009), VIMS spectral mapping observations of Titan during the Cassini prime mission, *Planet. Space Sci.*, *57*, 1950–1962.

Barnes, J. W., et al. (2011), Organic sedimentary deposits in Titan's dry lakebeds: Probable evaporite, *Icarus*, *216*, 136–140, doi:10.1016/j.icarus.2011.08.022.

Bray, V., et al. (2012), Ganymede crater dimensions—implications for central peak and central pit formation and development, *Icarus*, *217*, 115–129.

Brown, R. H., et al. (2004), The Cassini Visual and Infrared Mapping Spectrometer (VIMS) investigation, *Space Sci. Rev.*, *115*, 111–168.

Burr, D. M., R. M. E. Williams, K. D. Wendell, and J. P. Emery (2010), Inverted fluvial features in the Aeolis/Zephyria Plana region, Mars: Formation mechanism and initial paleodischarge estimates, *J. Geophys. Res.*, *115*, E07011, doi:10.1029/2009JE003496.

Chen, C. W., Hensley, S. (2005), Amplitude-based height-reconstruction techniques for synthetic aperture ladar systems, *J. Opt. Soc. Am. A*, *22* (3), 529–538.

Choukroun, M., O. Grasset, G. Tobie and C. Sotin (2010), Stability of methane clathrate hydrates under pressure: Influence on outgassing processes of methane on Titan, *Icarus*, *205*, 581–593.

Clark, R. N., et al. (2010), *J. Geophys. Res. (Planets)*, *115*, 28, E10005, doi:10.1029/2009JE003369.

Consani, K., G. C. Pimentel (1987), Infrared spectra of the clathrate hydrates of acetylene and acetylene/acetone, *J. Phys. Chem.*, *91*, 289–293.

Cottini, V., C. A. Nixon, D. E. Jennings, R. de Kok, N. A. Teanby, P. G. J. Irwin, and F. M. Flasar (2012), Spatial and temporal variations in Titan's

surface temperatures from Cassini CIRS observations, *Planet. Space Sci.*, *60*, 62–71.
Crawford, G. D., and D. J. Stevenson (1988), Gas-driven water volcanism and the resurfacing of Europa, *Icarus*, *73*, 66–79.
Croft, S. K., J. I. Lunine, and J. S. Kargel (1988), Equations of state of ammonia–water liquid: Derivation and planetological applications, *Icarus*, *73*, 279–293.
Croft, S. K. et al. (1995), Geology of Triton, in *Neptune and Triton*, edited by D. P. Cruikshank and M. S. Matthews, pp. 879–948, University of Arizona Press, Tucson.
Davies, A. G., C. Sotin, D. L. Matson, J. C. Castillo-Rogez, T. V. Johnson, M. Choukroun, and K. H. Baines (2010), Atmospheric control of the cooling rate of impact melts and cryolavas on Titan's surface, *Icarus*, *208*, 887–895, doi:10.1016/j.icarus.2010.02.025.
Elachi, C., et al. (2005), RADAR: The Cassini Titan Radar Mapper, *Space Sci. Rev. 117*, 71–110.
Elachi, C., et al. (2006), Titan Radar Mapper Observations from Cassini's Ta and T3 Fly-bys, *Nature*, *441/8*, 709–713, doi:10.1038/nature0486.
Fagents, S. A. (2003), Considerations for effusive cryovolcanism on Europa: The post-Galileo perspective, *J. Geophys. Res.*, *108*, E125139, doi:10.1029/2003JE002128.
Fagents, S. A., et al. (2000), Cryomagmatic mechanisms for the formation of Rhadamanthys Linea, triple band margins, and other low albedo features on Europa, *Icarus*, *144*, 54–88.
Fulchignoni, M., et al. (2005), In situ measurements of the physical characteristics of Titan's environment, *Nature*, *438*, 785–791, doi:10.1038/nature04314.
Grasset, O., and C. Sotin (1996), The cooling rate of a liquid shell in Titan's interior, *Icarus*, *123*, 101–112.
Grasset, O., C. Sotin, and F. Deschamps (2000), On the internal structure and dynamics of Titan, *Planet. Space Sci.*, *48*, 617–636.
Hayes, A G., et al. (2008a), Joint analysis of Titan's surface using the Cassini VIMS and Radar instruments, Division for Planetary Sciences annual meeting, Ithaca, abstract #34.06.
Hayes, A. G., et al. (2008b), Hydrocarbon lakes on Titan: Distribution and interaction with a porous regolith, *Geophys. Res. Lett.*, *35*, L09204, doi:10.1029/2008GL033409.
Hayes, A. G., et al. (2011), Transient surface liquids in Titan's polar regions from Cassini, *Icarus*, *211*, 655–671.
Head, J. W., and R. T. Pappalardo (1999), Brine mobilization during lithospheric heating on Europa: Implications for formation of chaos terrain, lenticula texture and color variations, *J. Geophys. Res.*, *104*, 27,143–27,155.
Head, J. W., and L. Wilson (1992), Magma reservoirs and neutral buoyancy zones on Venus: Implications for the formation and evolution of volcanic landforms, *J. Geophys. Res.*, *97*(E3), 3877–3903, doi:10.1029/92JE00053.
Iess, L., et al. (2012), The tides of Titan, *Science*, *1219631*, doi: 10.1126/science.1219631.
Janssen, M. A., et al. (2009), Titan's surface at 2.2-cm wavelength imaged by the Cassini RADAR Radiometer: Calibration and first results, *Icarus*, *200*, 222–239, doi:10.1016/j.icarus.2008.10.017.
Janssen, M. A., A. Le Gall, and R. Lopes (2011a), Looking for Thermal Anomalies on Titan's Surface. American Geophysical Union, Fall Meeting, 2011, San Francisco, abstract # P32C-04.
Janssen, M. A., A. Le Gall, and L. C. Wye (2011b), Anomalous radar backscatter from Titan's surface, *Icarus*, *212*, 321–328.
Jaumann, R., et al. (2008), Fluvial erosion and post-erosional processes on Titan, *Icarus*, *197*, 526–538, doi:10.1016/j.icarus.2008.06.002.
Jennings, D. E., et al. (2009), Titan's surface brightness temperatures, *Ap. J. L.*, *691*, L103–L105.
Kargel, J. S. (1992), Ammonia-water volcanism on icy satellites: Phase relations at 1 atmosphere, *Icarus*, *100*, 556–574.
Kargel, J. S. (1995), Cryovolcanism on the icy satellites, *Earth Moon Planets*, *67*, 101–113.
Kargel, J. S., and R. G. Strom (1990), Cryovolcanism on Triton, *Lunar and Planet. Sci. Conf.*, *XXI*, 599–600.
Kargel, J. S., S. Croft, J. Lunine, and J. Lewis (1991), Rheological properties of ammonia-water liquids and crystal slurries: Planetological implications, *Icarus*, *89*, 93–112.
Kargel, J. S., R. Furfaro, and P. Candelaria (2010), Distinct aqueous and hydrocarbon cryovolcanism on Titan and other icy satellites (invited), Am. Geophys. Union, Fall Meeting, 2010, San Francisco, abstract #P22A-02.
Kirchner, M. T., R. Boese, W. E. Billups, and L. R. Norman (2004), Gas hydrate single-crystal structure analyses, *J. Am. Chem. Soc.*, *126*, 9407–9412.
Kirk, R. L., and E. Howington-Kraus (2008), Radargrammetry on three planets, International Archives of Photogrammetry, Remote Sensing, and Spatial Information Sciences, XXXVII, Part 4, A Silk Road for Information from Imagery, Beijing, pp. 973–980.
Kirk, R. L., P. Callahan, R. Seu, R. D. Lorenz, F. Paganelli, R. M. Lopes, C. Elachi, and the Cassini Radar Team (2005), Radar reveals Titan topography. *Lunar Planet. Sci. XXXVI*, Abstract 2227.
Kirk, R. L., et al. (2008), A three-dimensional view of Titan's surface features from Cassini RADAR stereogrammetry, *Eos Trans. AGU*, *89*(53), *Fall Meet. Suppl.*, Abstract P11D-09.
Kirk, R. L., et al. (2009), Three-dimensional views of Titan's diverse surface features from Cassini RADAR stereogrammetry, *Lunar Planet. Sci.*, *XL*, Abstract #1413, Lunar and Planetary Institute, Houston (CD-ROM).
Kirk, R. L., E. Howington-Kraus, A. G. Hayes, R. M. C. Lopes, R. D. Lorenz, J. I. Lunine, K. L. Mitchell, E. R. Stofan, and S. D. Wall (2010), La Sotra y los otros: Topographic evidence for (and against) cryovolcanism on Titan, *Eos Trans. AGU*, *91*(52), *Fall Meet. Suppl.*, Abstract P22A-03.
Le Corre, L., et al. (2009), Analysis of a cryolava flow-like feature on Titan, *Planet. Space Sci.*, *57*, 870–879.
Le Gall, A., M. A. Janssen, R. D. Lorenz, P. Paillou, S. D. Wall and the Cassini Radar Team (2010), Radar-bright channels on Titan, *Icarus*, *207*, 948–958.
Le Gall, A., A. G. Hayes, R. Ewing, M. A. Janssen, J. Radebaugh, C. Savage, P. Encrenaz and the Cassini Radar Team (2012), Latitudinal and altitudinal controls of Titan's dune field morphometry, *Icarus*, *217*, 231–242.
Le Mouelic, S., et al. (2008), Mapping and interpretation of Sinlap crater on Titan using Cassini VIMS and RADAR data, *J. Geophys. Res.*, *113*, doi:10.1029/2007JE002965.
Lopes, R. M. C., and Kilburn, C. R. J. (1990), Emplacement of lava flows fields: Application of terrestrial studies to Alba Patera, Mars, *J. Geophys. Res.*, *95*(B9), 14,383–14,397.
Lopes, R. M. C., et al. (2007), Cryovolcanic features on Titan's surface as revealed by the Cassini Titan Radar Mapper, *Icarus*, *186*, 395–412.
Lopes, R. M. C., et al. (2010a), Distribution and interplay of geologic processes on Titan from Cassini RADAR data, *Icarus*, *205*, 540–588, doi:10.1016/j.icarus.2009.08.010.
Lopes, R. M. C., K. L. Mitchell, D. A. Williams, and G. Mitri (2010b), Beyond Earth: How extra-terrestrial volcanism has changed our definition of a volcano, in *What's a Volcano? New Answers to an Old Question*, edited by E. Canon and A. Szakacs, pp. 11–30, Geological Society of America Special Paper 470, Geological Society of America, Inc., Boulder, Colo.
Lopes, R. M., et al. (2011), Interpreting Titan's surface geology from Cassini RADAR observations, American Geophysical Union Fall Meeting.
Lorenz, R. D. (1996), Pillow lava on Titan: Expectations and constraints on cryovolcanic processes, *Planet. Space Sci.*, *44*, 1021–1028.
Lorenz, R., and J. Mitton (2002), *Lifting Titan's Veil*, 260 pp. Cambridge University Press, Cambridge, U. K.
Lorenz, R. D., G. Builloz, P. Encrenaz, M. A. Janssen, R. D. West, and D. O. Muhleman (2003), Cassini Radar: Prospects for Titan surface investigations using the microwave radiometer, *Planet. Space Sci.*, *51*, 353–364.
Lorenz, R. D., et al. (2008), Fluvial channels on Titan: Meteorological paradigm and Cassini RADAR observations, *Planet. Space Sci.*, *56*, 1132–1144.
Manga, M., and C. Y. Wang (2007), Pressurized oceans and the eruption of liquid water on Europa and Enceladus, *Geophys. Res. Lett.*, *34*, L07202, doi:10.1029/2007GL029297.
Marion, G., J. S. Kargel, D. C. Catling, and J. I. Lunine (2012), Ammonia-ammonium aqueous chemistries in the solar system's icy bodies, *Icarus 220*, 932–946, doi:10.1016/j.icarus.2012.06.016.
McCord, T. B., et al. (2008), Titan's surface: Search for spectral diversity and composition using the Cassini VIMS investigation, *Icarus*, *194*, 212–242.
McKinnon, W. B. (2006), On convection in ice I shells of outer solar system bodies, with detailed application to Callisto, *Icarus*, *183*, 435–450.
McKinnon, W. B. (2010), Argon-40 degassing from Titan and Enceladus: A tale of two satellites, 41st Lunar Planetary Science Conference, abstract #2718.
Mitchell, K. L., and M. Malaska (2011), Karst on Titan, First International Planetary Cave Research Workshop, October 2011, Carlsbad, New Mexico, Abstract #8021.
Mitri, G., and A. P. Showman (2005), Convective-conductive transitions and sensitivity of a convecting ice shell to perturbations in heat flux and tidal-heating rate: Implications for Europa, *Icarus*, *177*, 447–460.
Mitri, G., and A. P. Showman (2008), A model for the temperature-dependence of tidal dissipation in convective plumes on icy satellites: Implications for Europa and Enceladus, *Icarus*, *195*, 758–764.
Mitri, G., J. I. Lunine, A. P. Showman, and R. Lopes (2008), Resurfacing of Titan by ammonia-water cryomagma, *Icarus*, *196*, 216–224, doi:10.1016/j.icarus.2008.02.024.

Moore, J. M., and A. D. Howard (2010), Are the basins of Titan's Hotei and Tui Regio sites of former low latitude seas? *Geophys. Res. Lett.*, *37*, L22205, doi:10.1029/2010GL045234.

Moore, J. M., and R. T. Pappalardo (2011), Titan: An exogenic world? *Icarus*, *212*, 790–806.

Neish, C. D., Lorenz, R. D., Kirk, R. L., and Wye, L. C. 2010. Radarclinometry of the sand seas of Africa's Namibia and Saturn's moon Titan, *Icarus*, *208*, 385–394.

Neish, C. D., R. L. Kirk, R. D. Lorenz, V. J. Bray, P. Schenk, B. Stiles, E. Turtle, K. Mitchell, A. Hayes, and the Cassini RADAR Team (2013), Crater topography on Titan: Implications for landscape evolution, *Icarus*, *223*, 82–90, doi:10.1016/j.icarus.2012.11.030.

Nelson, R. M., et al. (2009a), Saturn's Titan: Surface change, ammonia, and implications for atmospheric and tectonic activity, *Icarus*, *199*, 429–441, doi:10.1016/j.icarus.2008.08.013.

Nelson, R. M., et al. (2009b), Photometric changes on Saturn's moon Titan: Evidence for cryovolcanism, *Geophys. Res. Lett.*, *36*, L04202, doi:10.1029/2008GL036206.

Nichols, G. (2009), *Sedimentary and Stratigraphy*, 2nd ed., 432 pp., Wiley-Blackwell, Maiden, Mass., Oxford, U. K., and Carlton, Australia.

Niemann, H. B., et al. (2005), Huygens Probe Gas Chromatograph Mass Spectrometer: The atmosphere and surface of Titan, *Nature*, doi:10.1038/nature04122.

Niemann, H. B., S. K. Atreya, J. E. Demick, D. Gautier, J. A. Haberman, D. N. Harpold, W. T. Kasprzak, J. I. Lunine, T. C. Owen, and F. Raulin (2010), Composition of Titan's lower atmosphere and simple surface volatiles as measured by the Cassini-Huygens probe gas chromatograph mass spectrometer experiment, *J. Geophys. Res.*, *115*, E12006 doi: http://dx.doi.org/10.1029/2010JE003659.

Nimmo, F., and B. G. Bills (2010), Shell thickness variations and the long-wavelength topography of Titan, *Icarus*, *208*, 896–904, doi:10.1016/j.icarus.2010.02.020.

Ostro, S. J., et al. (2006), Cassini RADAR observations of Enceladus, Tethys, Dione, Rhea, Iapetus, Hyperion, and Phoebe, *Icarus*, *183*, 479–490.

Paganelli, F., et al. (2005), Channels and fan-like features on Titan's surface imaged by the Cassini RADAR, Proc. Lunar Planet. Sci. Conf. 36th, Abstract 2150.

Pain, C. F., J. D. A. Clarke, and M. Thomas (2007), Inversion of relief on Mars, *Icarus*, *190*, 478–491, doi:10.1016/j.icarus.2007.03.017.

Porco, C. C., et al. (2006), Cassini observes the active south pole of Enceladus, *Science*, *311*(5766), 1393–1401, doi:10.1126/science.1123013.

Prockter, L. (2004), Ice volcanism on Jupiter's moons and beyond, in *Volcanic Worlds: Exploring the Solar System Volcanoes*, edited by R. Lopes and T. K. Gregg, pp. 145–177, Praxis Publishing Company (Springer-Verlag), Chichester, U. K.

Radebaugh, J., R. Lorenz, R. Kirk, J. Lunine, E. Stofan, R. Lopes, S. Wall, and the Cassini Radar Team (2007), Mountains on Titan observed by Cassini RADAR, *Icarus*, *192*, 77–91, doi:10.1016/j.icarus.2007.06.020.

Radebaugh, J., et al. (2008), Dunes on Titan observed by Cassini RADAR, *Icarus*, *194*, 690–703, doi:10.1016/ j.icarus.2007.10.01janssen.

Radebaugh, J., et al. (2010), Regional geomorphology and history of Titan's Xanadu province, *Icarus*, doi:10.1016/j.icarus.2010.07.022.

Rannou, P., F. Hourdin, and C. P. McKay (2002), A wind origin for Titan's haze structure, *Nature*, *418*(6900), 853–856.

Rodriguez, S., et al. (2006), Cassini/VIMS hyperspectral observations of the Huygens landing site on Titan, *Planet. Space Sci.*, *54*, 1510–1523.

Schenk, P. (2002), Thickness constraints on the icy shells of the Galilean satellites from a comparison of crater shapes, *Nature*, *417*, 419–421.

Showman, A. P., I. Mosqueira, and J. W. Head (2004), On the resurfacing of Ganymede by liquid-water volcanism, *Icarus*, *172*, 625–640.

Soderblom, L., et al. (2007), Correlations between Cassini VIMS spectra and RADAR SAR images: Implications for Titan's surface composition and the character of the Huygens Probe landing site, *Planet. Space Sci.*, *55*, 2025–2036.

Soderblom, L. A., et al. (2009), The geology of Hotei Regio, Titan: Correlation of Cassini VIMS and RADAR, *Icarus*, *204*, 610–618, doi:10.1016/j.icarus.2009.07.033.

Soderblom, J. M., et al. (2010), Geology of the Selk Crater Region on Titan from Cassini VIMS observations, *Icarus*, *208*, doi:10.1016/j.icarus.2010.03.001.

Sotin, C., et al. (2005), Release of volatiles from a possible cryovolcano from near-infrared imaging of Titan, *Nature*, *435*, 786–789.

Sotin, C., R. H. Brown, K. Lawrence, S. LeMouelic, J. Barnes, J. Soderblom, and the VIMS Team (2010), High resolution mapping of Titan with VIMS, EPSC abstracts, vol. 5, EPSC2010-856, European Planetary Science Congress.

Spencer, J. R., J. C. Pearl, M. Segura, F. M. Flasar, A. Mamoutkine, P. Romani, B. J. Buratti, A. R. Hendrix, L. J. Spilker, and R. M. C. Lopes (2006), Cassini finds Enceladus is active: Background, and Composite Infrared Spectrometer (CIRS) observations of a south polar hot spot, *Science*, *311*, 1401–1405.

Stevenson, D. J. (1992), Interior of Titan, in *Proceedings Symposium on Titan*, Toulouse, France, 912 September 1991, pp. 2933, European Space Agency, Noordwijk, the Netherlands.

Stiles, B. W., et al. (2009), Determining Titan surface topography from Cassini SAR data, *Icarus*, *202*, 584–598.

Stofan, E. R., et al. (2006), Mapping of Titan: Results from the first two Titan Radar passes, *Icarus*, *185*(2), 443–456.

Stofan, E. R., et al. (2009), Morphology of four flow fields on Titan: Implications for modes or origin, Lunar Planet. Sci. Conf. 40th, abstract # 1043.

Tobie, G., O. Grasset, J. I. Lunine, A. Mocquet, and C. Sotin (2005), Titan's internal structure inferred from a coupled thermal-orbital model, *Icarus*, *175*, 496–502.

Tobie, G., O. Čadek, and C. Sotin (2008), Solid tidal friction above a liquid water reservoir as the origin of the south pole hotspot on Enceladus, *Icarus*, *196*, 642–652.

Toon, O. B., R. P. Turco, and J. B. Pollack (1980), A physical model of Titan's clouds, *Icarus*, *43*, 260–282.

Wall, S. D., et al. (2009), Cassini RADAR images at Hotei Arcus and Western Xanadu, Titan: Evidence for recent cryovolcanic activity, *Geophys. Res. Lett.*, *36*, L04203, doi:10.1029/2008GL036415.

Wood, C. A. (2011), Bipolar volcanism on Titan? 42nd Lunar and Planetary Science Conference, #1313.

Wye, L. (2011), Radar scattering from Titan and Saturn's icy satellites using the Cassini spacecraft, Ph.D. Thesis, Stanford University.

Yung, Y. L., M. Allen, and J. P. Pinto (1984), Photochemistry of the atmosphere of Titan: Comparison between model and observations, *Astrophys. J. Suppl. Ser.*, *55*, 465–506.

Zhong, F., K. Mitchell, C. Hays, M. Choukroun, M. Barmatz, and J. Kargel (2009), The rheology of cryovolcanic slurries: Motivation and phenomenology of methanol-ethanol-water slurries with implications for Titan, *Icarus*, *202*, 607.